



**Michigan  
Technological  
University**

Michigan Technological University  
**Digital Commons @ Michigan Tech**

---

Dissertations, Master's Theses and Master's Reports

---

2017

## **Minimizing Run Time of Finite Element Analyses: Applications in Conformable CNG Tank Modeling**

Paul M. Roehm

*Michigan Technological University*, pmroehm@mtu.edu

Copyright 2017 Paul M. Roehm

---

### **Recommended Citation**

Roehm, Paul M., "Minimizing Run Time of Finite Element Analyses: Applications in Conformable CNG Tank Modeling", Open Access Master's Report, Michigan Technological University, 2017.

<https://doi.org/10.37099/mtu.dc.etr/380>

Follow this and additional works at: <https://digitalcommons.mtu.edu/etr>



Part of the [Computer-Aided Engineering and Design Commons](#)

MINIMIZING RUN TIME OF FINITE ELEMENT ANALYSES:  
APPLICATIONS IN CONFORMABLE CNG TANK MODELING

By

Paul M. Roehm

A REPORT

Submitted in partial fulfillment of the requirements for the degree of

MASTER OF SCIENCE

In Mechanical Engineering

MICHIGAN TECHNOLOGICAL UNIVERSITY

2017

© 2017 Paul Roehm

This report has been approved in partial fulfillment of the requirements for the Degree of MASTER OF SCIENCE in Mechanical Engineering.

Department of Mechanical Engineering-Engineering Mechanics

Report Advisor: *Dr. Gregory Odegard*

Committee Member: *Dr. Paulus van Susante*

Committee Member: *Dr. Adam Loukus*

Department Chair: *Dr. William Predebon*

# Table of Contents

Abstract.....	vi
<b>1. Introduction.....</b>	<b>1</b>
<b>1.1 Project Overview.....</b>	<b>1</b>
<b>1.2 Background.....</b>	<b>1</b>
<b>1.2.1 Alternative Fuels.....</b>	<b>1</b>
<b>1.2.2 State of the Art: CNG Tanks.....</b>	<b>2</b>
<b>1.2.3 REL Conformable Tank.....</b>	<b>3</b>
<b>1.2.4 Large Models of Complex Geometry.....</b>	<b>4</b>
<b>1.3 Mechanical Testing Standards: NGV2.....</b>	<b>4</b>
<b>1.3.1 Burst Testing.....</b>	<b>5</b>
<b>1.3.2 Drop Testing.....</b>	<b>5</b>
<b>2. Problem Analysis.....</b>	<b>7</b>
<b>2.1 Project Goal.....</b>	<b>7</b>
<b>2.2 Project Objectives.....</b>	<b>7</b>
<b>2.3 Limitations.....</b>	<b>7</b>
<b>3. Geometry and Material Models.....</b>	<b>8</b>
<b>3.1 Tank Geometry.....</b>	<b>8</b>
<b>3.2 Concrete Floor Geometry.....</b>	<b>9</b>
<b>3.3 Aluminum Material Model.....</b>	<b>11</b>
<b>3.4 Concrete Material Model.....</b>	<b>13</b>
<b>4. Mesh Selection.....</b>	<b>14</b>

4.1 Shell v. Solid Elements (First Order).....	14
5. Static Modeling – Starting Mesh Size Determination.....	15
5.1 Static Model Overview – Boundary Conditions.....	15
5.1.1 Static Displacement Constraints.....	15
5.1.2 Static Loading Conditions.....	16
5.2 Static Convergence Criteria.....	16
5.3 Static Analysis Results.....	17
6. Dynamic Modeling – Convergence Verification.....	20
6.1 Dynamic Model Overview – Boundary Conditions.....	21
6.1.1 Dynamic Displacement Constraints.....	21
6.1.2 Dynamic Loading Conditions.....	22
6.1.3 Dynamic Contact Controls.....	23
6.2 Dynamic Convergence Criteria.....	23
6.3 Dynamic Analysis Results.....	24
6.4 Physical Validation.....	28
7. Time Reduction Methods.....	30
7.1 Symmetrical Building Block.....	30
7.2 Gradient Meshing.....	32
7.3 Hybrid Element Meshing.....	32
7.4 Planes of Symmetry.....	33
7.5 2 <sup>nd</sup> Order Elements.....	33
7.6 Rigid Wall.....	34

<b>8. Dynamic Modeling – Runtime Reduction Testing.....</b>	<b>34</b>
<b>8.1 Symmetric Building Block Analysis.....</b>	<b>35</b>
<b>8.2 Gradient Mesh Analysis.....</b>	<b>37</b>
<b>8.3 Hybrid Mesh Analysis.....</b>	<b>39</b>
<b>9. Conclusions and Recommendations.....</b>	<b>43</b>
<b>10. Potential Future Work.....</b>	<b>44</b>
<b>References.....</b>	<b>46</b>

## **Abstract**

REL Inc. has proposed a CNG tank that deviates from typical cylindrical storage methods. The goal of REL working with Michigan Tech is to minimize mass and meet NGV2 safety standards for pressure and drop testing for this tank.

The model has undulated outer surfaces and Schwarz P-surface internal geometry. To accurately mesh this, a small element size is necessary; this creates a model with millions of elements. In explicit analyses, this requires a large amount of computational resources to run.

This report focuses on methods to reduce model run time without reducing accuracy. Methods covered include creating symmetric building blocks, gradient meshing, and hybrid (shell to solid) meshing. Results indicate that building block and gradient methods reduce run time by 84% and 78% respectively for an accuracy cost below 5%. Hybrid meshing shows a potential of 50% additional reduction but element formulation must be changed to reduce accuracy cost.

# **1. Introduction**

## **1.1. Project Overview**

REL, Inc. needs to optimize a conformable compressed natural gas (CNG) tank to minimize mass while meeting national safety standards. Instead of creating a large number of physical models and going through an excess of tooling and molding equipment, it is cost effective to simulate these standards using finite element analysis (FEA). While many FEA models for optimization have a short runtime due to low number of equations (few nodes) or have a large timestep in dynamic simulations, the CNG tank requires a large number of elements with a small timestep. Additionally, future CNG tank model CAD is predicted to increase in size by a factor of 3.5. Therefore it is critical to explore methods to reduce the runtime of CNG tank models while maintaining model accuracy. This report is focused on exploring these methods and recommending a course of action for future modeling attempts.

## **1.2. Background**

### **1.2.1. Alternative Fuels**

Alternative fuels are a rising interest worldwide – as such, vehicle technology has started to shift focus toward fuels that replace traditional gasoline. This is especially prevalent in the public transportation sector, where it is reported that, as of 2013, over 35% of U.S public buses are using “alternative fuels or hybrid technology” to reduce emissions. [1] This growth is also being incentivized by the US government. Congress has continued to extend the Protecting Americans from Tax Hikes (PATH) Act which provides tax benefits for CNG and liquefied natural gas (LNG). [2]

Alternative fuels are defined by the lack of gasoline and therefore include a broad set of fuel types. In the transportation sector leading fuel types include biodiesel, ethanol, electric, natural gas (CNG or LNG), and hydrogen. Figure 1 shows the number of vehicles made for different fuel types between 2004 and 2015.



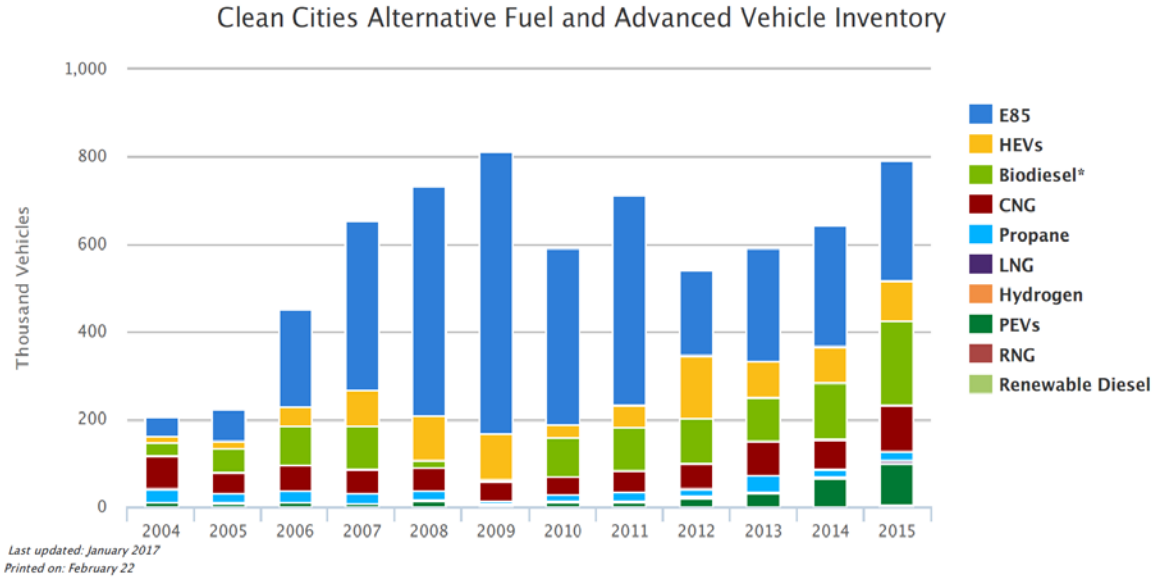


**Figure 1:** Growth of Alternative Fuels Vehicles in the Transportation Sector from 2004 to 2015 [3]

Ethanol 85 (E85) and Hybrid Electric Vehicles (HEVs) both utilize petroleum gas. Without these two components, the leading alternative fuel vehicles as of 2015 are biodiesel, followed by CNG and Plug-in Electric Vehicles (PEVs).

Focusing on natural gas, this fuel is highly available and is mass produced in the US. As such it is easily accessible to the public. In addition to this, it is a clean-burning fuel and provides similar “power, acceleration and cruising speed” compared to gasoline. The current downside of using natural gas is that the total mileage a vehicle can travel before refilling is reduced. [4]

In terms of manufacturing, CNG is simple to produce. Natural gas is compressed in a range of 3000-3600 psi to a volume less than 1% what the free gas would take. Conversely, LNG production requires cryogenic tanks and storage at a temperature of -260°F [4]. Natural gas is therefore most accessible as a fuel in CNG form at this time.

### 1.2.2. State of the Art: CNG Tanks

The typical state of CNG tanks is the rounded cylinder shown in Figure 2.



**Figure 2:** Type 3 Cylindrical CNG Tank [5]

There are currently 4 types of CNG tank. As the type number increases the typical weight decreases. Type 1 tanks are a formed steel or aluminum which typically have a protective coating around them. Type 2 tanks use a steel liner around the volume which is surrounded by a partial composite material ‘wrap’ in the middle of the tank. Type 3 tanks are typically made with an aluminum liner and a full composite wrap (ex. carbon fiber). Type 4 tanks have no metal, instead using plastic with a rubber liner and a composite wrap around the natural gas. [6] [7]

The cylindrical tank geometry removes stress concentrations that would occur at sharp corners. However, when mounting the cylinders, the geometry makes it difficult to place the tanks on vehicles without a fixture that accounts for the circular cross section. Therefore the tanks are typically placed in the back of truck beds, in trunks of cars, or on top of buses. Of these options, only buses have an option that does not remove available vehicle space. Additionally, because the fixtures must account for the circular cross section, the true packaging space for the tank is a rectangular cross section along its length. Therefore there is a motivation to find a tank design that uses this space and can be mounted more conveniently on vehicles.

### **1.2.3. REL Conformable Tank**

The CNG tank proposed by REL Inc. changes the tank structure to fit the packaging space. The current iteration (phase 1) of the tank is a cube as shown in the REL brochure image of Figure 3. This tank is considered a ‘modified type 1’ tank.

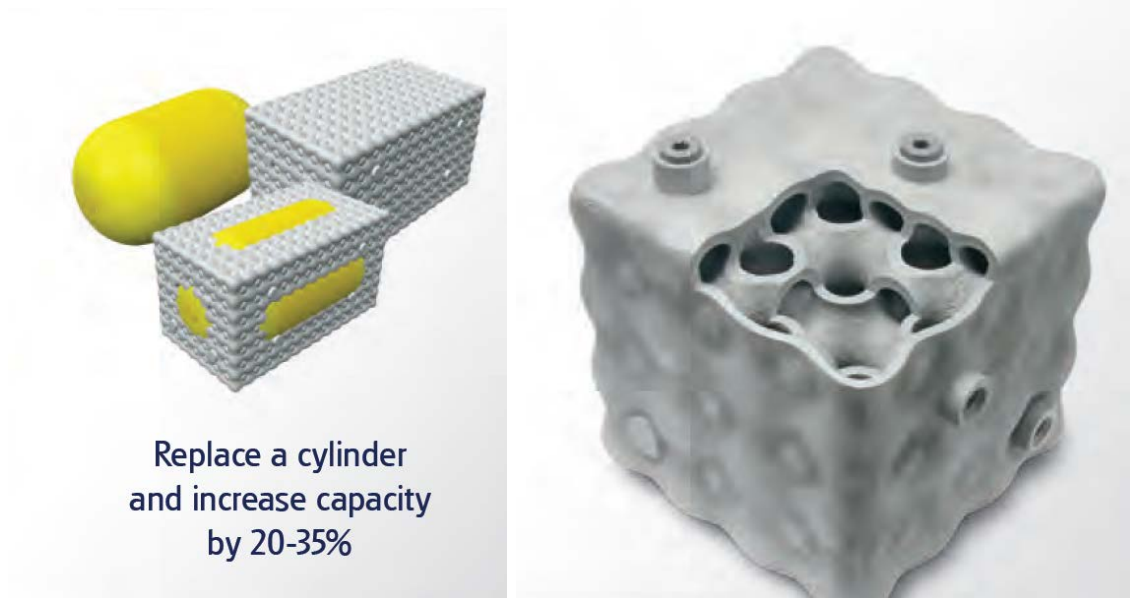


**Figure 3:** REL Modified Type 1 Conformable CNG Tank showing Additional Volumetric Storage (left) and Internal Structure (right) [8]

The tank offers an increase in CNG storage and a more convenient mounting shape by using radiused corners for the external surfaces and Schwarz P-surfaces for the internal geometry. These tanks are called ‘conformable tanks’ because they are not limited to a cube, but can instead form shapes around key components on vehicles or mounting brackets.

#### **1.2.4. Large Models of Complex Geometry**

As shown in Figure 3, the internal geometry of the tank is small and complex relative to the size of the tank and uses various radii throughout. It therefore requires a large number of small elements to properly model. Typically, small elements are associated with a small timestep in explicit analyses and require a large number of equations to solve in both implicit and explicit analyses. The typical approach to model a complex geometry is to construct a low runtime model (typically using a coarse mesh with the same boundary conditions) then increase mesh quality and test for convergence at increasingly small element sizes. This method aims to determine the minimum required size for an accurate analysis.

### **1.3. Mechanical Testing Standards: NGV2**

FEA test conditions for these tanks follows the NGV2 national safety standard. NGV2 standards cover a large number of tests that include but are not limited to: bonfire testing of the pressure relief device (PRD), exposure to corrosive chemicals, burst testing, cycle testing (type 4 only), drop testing, and bullet penetration testing. [9] While all of these

standards must be met, the focus of this research is the high-stress, non-fracture testing scenarios. These tests include burst and drop testing.

Because drop testing should cause the highest stress concentrations and requires dynamic simulation, this test method is the primary focus for this report. Pressure testing conditions are only used to determine a starting point for drop test simulations.

It should be noted that physical v. simulated NGV2 test standards are not the focus of this work. This report is not directly concerned with a model that exactly matches the expected strains within these tank simulation. Instead, the report focuses on assessing a ‘generally accurate’ model to discern runtime reduction methods. As such, NGV2 standards are only referenced for completeness and an understanding of where the load and boundary conditions originate. Further discussion on defining the ‘general accuracy’ of the simulations is discussed in the *Physical Validation* section of the dynamic modeling results.

### 1.3.1. Burst Testing

NGV2 burst testing requirements focus on internal pressurization of the CNG tank. The NGV2 standard assumes an operating pressure of 3000-3600 psi and burst (failure) pressure of 2.25 times the operating pressure. A sketch of the general load case for REL’s CNG tanks is shown in Figure 4.

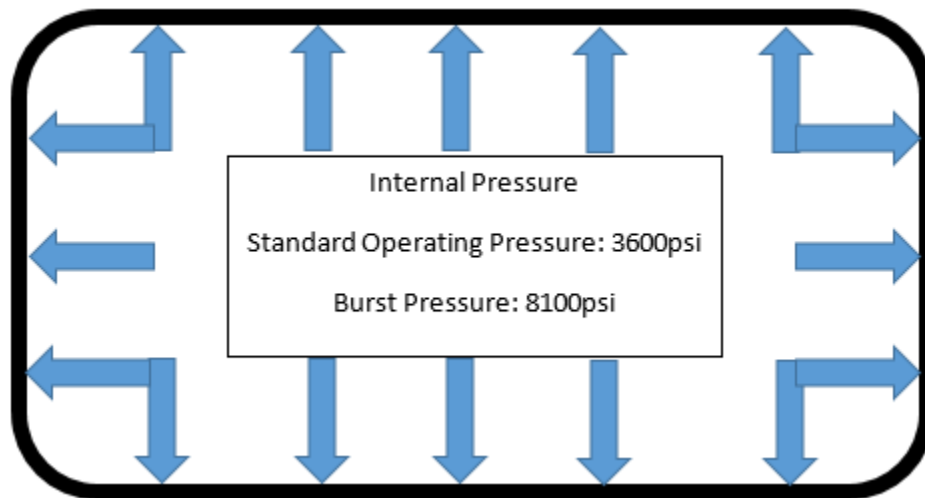


**Figure 4:** NGV2 Burst Pressure Test - Loading Conditions

### 1.3.2. Drop Testing

NGV2 drop test requirements have 2 drop test scenarios: a horizontal drop test and a 45° rotation drop test. The horizontal drop test involves the tank being dropped on its side from a height of 72” onto concrete. After the drop test, the tank must be pressure cycled from 10% to 125% of standard operating pressure for 3000 cycles without failure. The

45° rotation drop test is identical to the horizontal drop test except that the center of gravity (CG) of the tank must be at a height of 72" (or higher) and the tank is rotated 45°. [9] Both test conditions are shown in Figure 5.

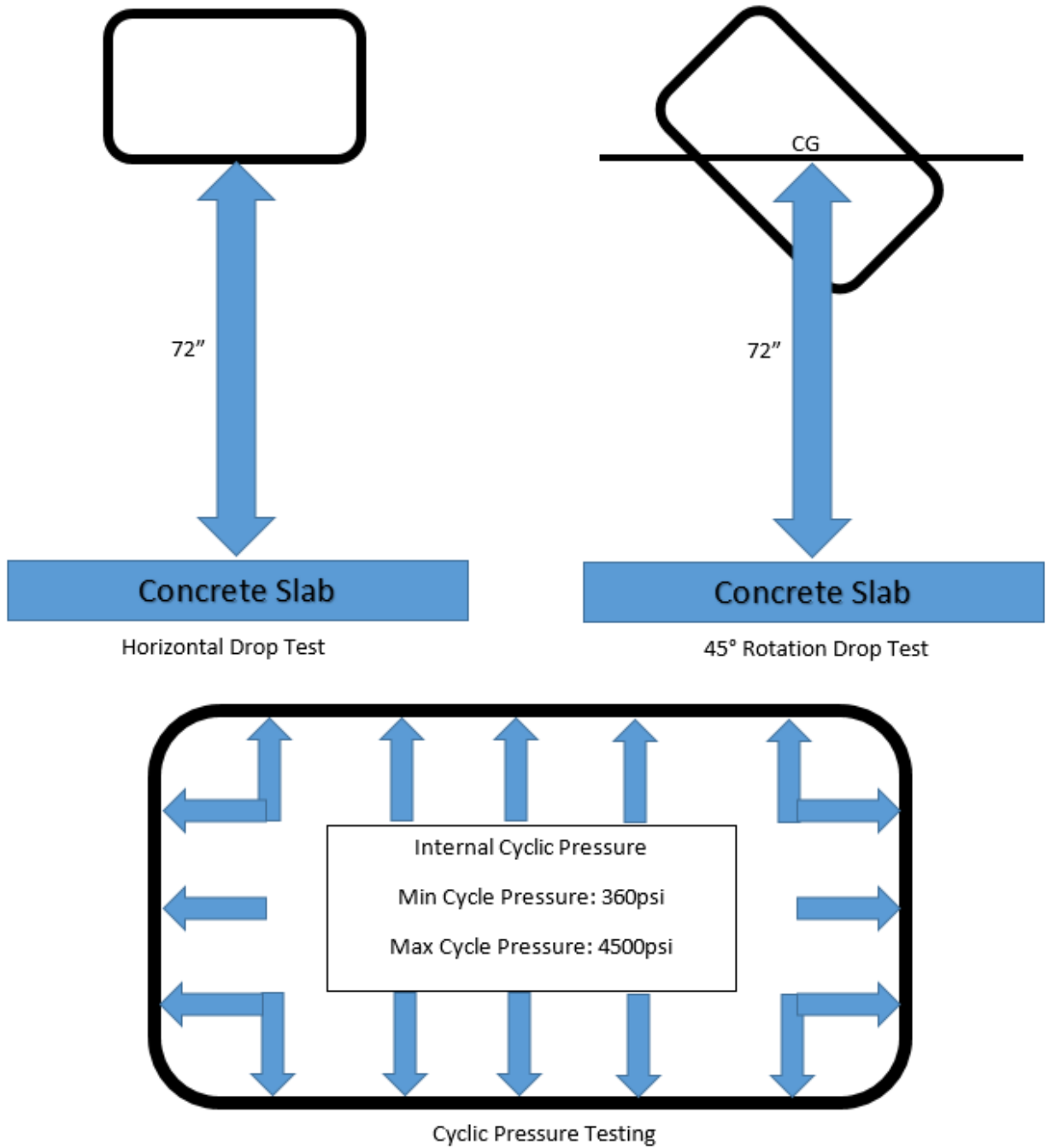


**Figure 5:** NGV2 Drop Test Configurations for Horizontal and 45° Impact

Note that Figure 5 shows an exaggerated size of the current iteration of CNG tanks. The decrease in height to initial impact in the 45° rotation configuration is not this large. However, in the case that the height decrease is significant, the tank must be rotated such that there is a minimum height of 24” and the CG is still at 72” above the ground. The internal pressure of the tank for these tests should be 0 psi (empty) and dropped at ambient temperature. [9]

## **2. Problem Analysis**

### **2.1. Project Goal**

The goal of the project is to recommend a method or set of methods that reduce current model run time while maintaining model accuracy. The model run time is monitored by CPU time taken by the simulation, while the model accuracy is measured by convergence compared to a baseline simulation. Note that convergence has multiple measures that must be considered. Acceptable percentile differences are further discussed in the associated analysis sections.

### **2.2. Project Objectives**

The project objectives to meet are:

- Determine a valid starting mesh size via static pressure analysis (implicit)
- Use converged static mesh size as a basis for dynamic impact convergence study (explicit)
- Test timestep reduction methods and compare convergence to the baseline. Use the converged dynamic impact model as this baseline.

These objectives were chosen to form a general method for replication and model formation if and/or when new CNG tank designs are created. The final objective is the critical piece of this report that directly answers the project goal. Note that validating a converged mesh size should, in future, also include physical strain comparisons on a model to further prove convergence. Since no strain data is known for drop test scenarios at this time, this step was not available.

### **2.3. Limitations**

Limitations of this project are runtime based. For the scope of this paper, all runs are performed on Michigan Technological University’s SUPERIOR cluster with 4 processors. Even so, runs take up to ~17 hours. Therefore, a general upper limit of 12 hours was set to determine a lower bound of element size for baseline models in impact. Considering phase 2 tanks are projected to increase the number of elements by a factor of 3.5, this would increase the runtime to ~42 hours per run. This time could increase depending on quality of elements and any additional contact between parts in future models. Running iterative mass optimization or full vehicle impact on models this large would be too time consuming to make the process worth it.

This limitation constrains both the timestep and element size (aka number of equations in the solver). Since the contact conditions given in the dynamic impact test case are simple, the timestep is directly related to the element size, and therefore directly constrains the minimum element size. If these results are replicated without use of SUPERIOR, element sizes that require a large runtime may need to be removed from the analyses.

### 3. Geometry and Material Models

#### 3.1. Tank Geometry

The tank geometry used in this report is a phase 1 tank. These tanks have a cubic shape. As mentioned in the *REL: Conformable Tank* section, the internal geometry of the tank is formed by Schwarz P-surfaces, a minimal surface designed with no edges. The external surface is undulated to reduce tank mass (as opposed to a flat surface). An image of the phase 1 CNG tank as-imported to HyperMesh is shown in Figure 6.

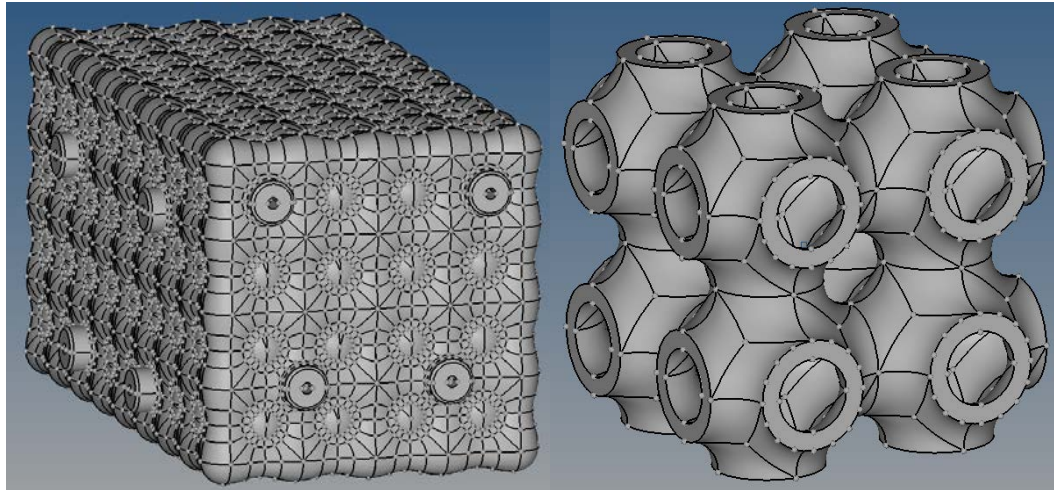


**Figure 6:** Imported Entire Tank (left) and Internal Geometry (right) of a Phase 1 Tank

While the tank itself is formed symmetrically, the geometric lines seen in the left image of Figure 6 do not allow for symmetry of the elements without a large amount of ‘line toggling’. In this process the user manually removes geometric lines from the model to re-impose symmetry and improve mesh quality.

Another critical point in the geometry is the ‘3-radius interface’, where 3 different radii come together in the geometry. This location occurs at every connection between the external and internal geometry as shown in Figure 7.



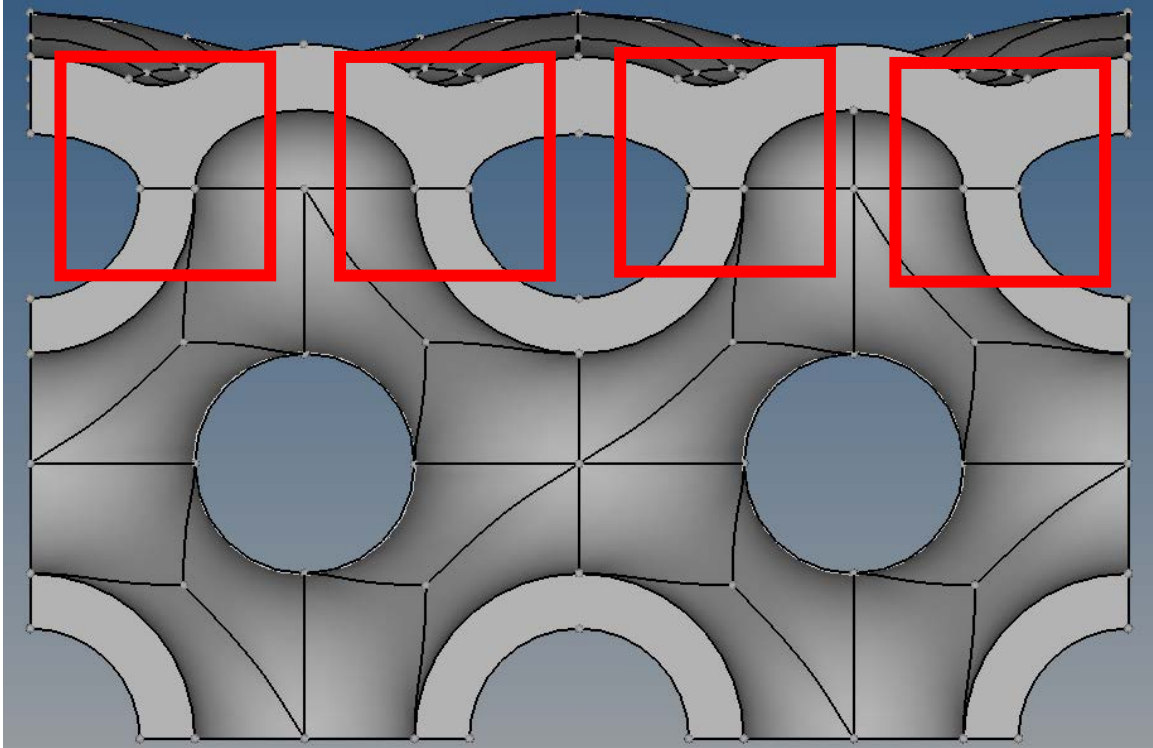


**Figure 7: 3-Radius Interface Location in CNG Tank**

This location has significance in element type selection and is further discussed in the *Shell v. Solid Elements (First Order)* section.

Finally, it is important to note that this geometry is not the only type that the methods described in this paper have been used for during research. Additional models include prototype phase 2 models, fork truck tank models, and flat external surface models.

### **3.2. Concrete Floor Geometry**

Floor geometry was used for dynamic impact analysis only. The width, length and thickness of the slabs at REL. Inc. were given as 5' x 5' x 6" and is within the typical precast concrete dimensions from online research. [10] A visual of the concrete dimensions are given in Figure 8.



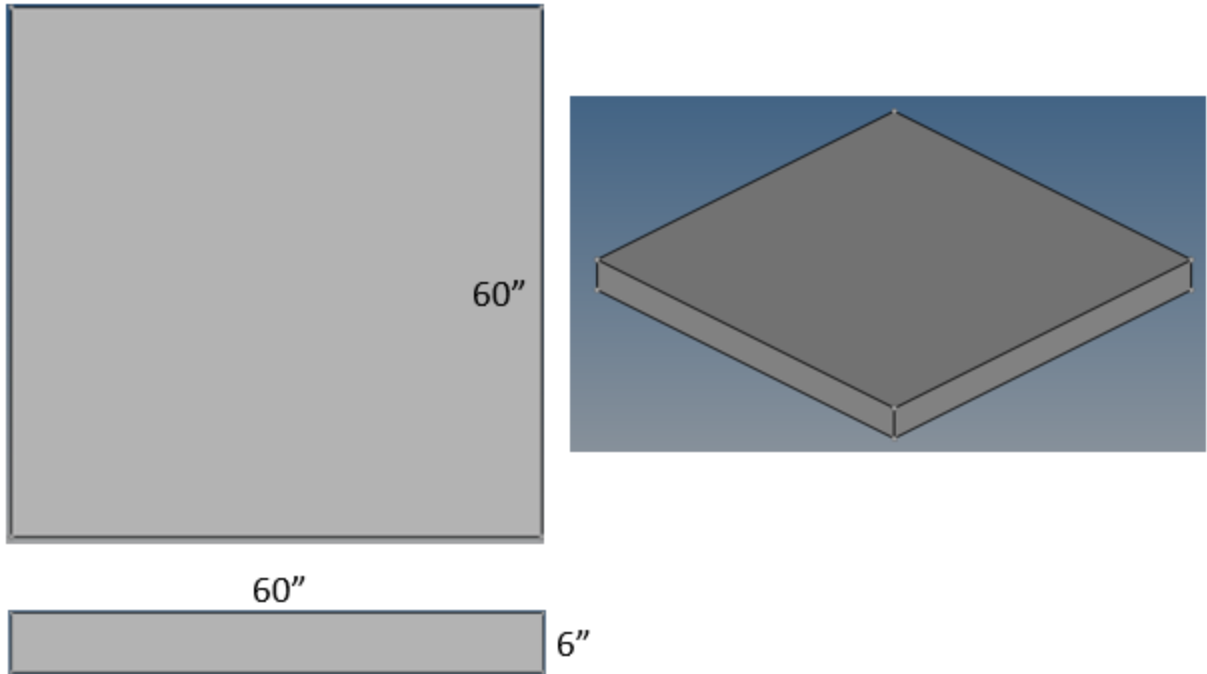


**Figure 8:** Concrete Slab Geometry with Front (bottom left), Top (top left) and Isometric (right) Views

For consistency with the modeling units used in this research (kg, mm, ms), the model dimensions in mm are 152.4 x 1524 x 1524 mm.

While concrete dimensions may vary between test locations in physical testing, the general dimensions are only necessary to have a realistic concrete impact surface. As long as the bending moment placed upon the concrete slab is relatively small (aka impose small displacement of concrete), user defined dimensions should be appropriate for the impact model. Note that there is a threshold at which small concrete plates without fracture mechanisms will create a much higher effective stiffness of the concrete. Similarly, using a larger concrete floor may reduce simulation noise (good for convergence) at the cost of model realism.

For completeness of potential concrete floor geometry, an alternate geometry is possible – a rigid wall. This method assumes the concrete absorbs no energy and is simply an impact surface for the CNG tank. Further information on the impact of using a rigid wall can be found in the *Rigid Wall* section.

### 3.3. Aluminum Material Model

The material used for these CNG tanks is A206 aluminum. The heat treatment options considered during this research include hot isostatic pressing (HIP), solution heat treated and natural aging (T4), and solution heat treated and artificial aging (T6). This report focuses on a T6 aging condition. The tensile curve and general material parameters are given in Figure 9 and Table 1 respectively.

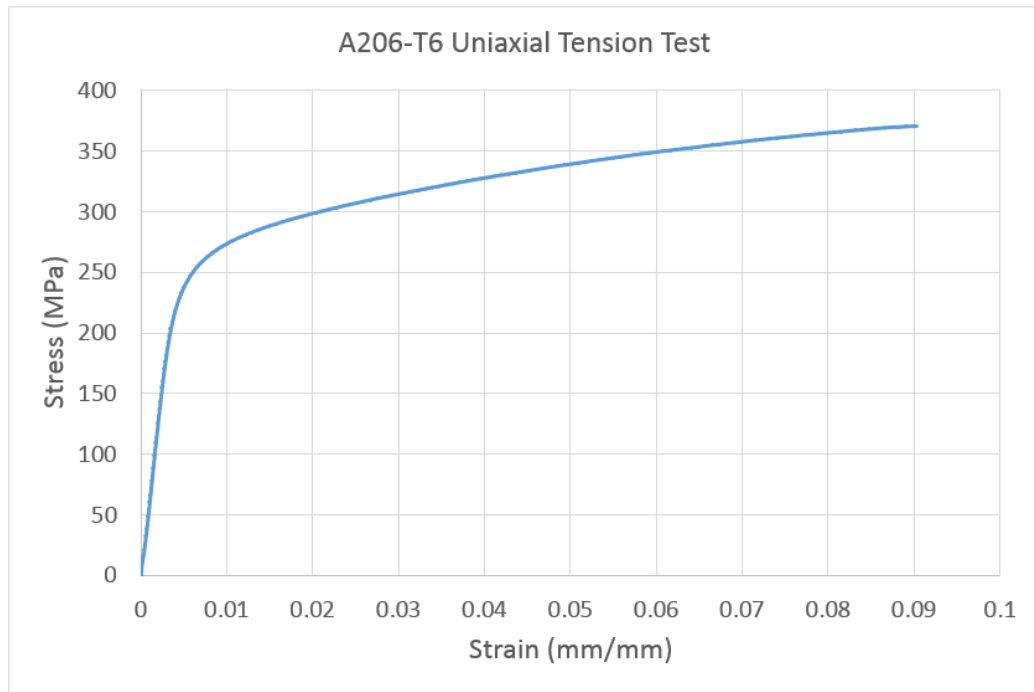


**Figure 9:** Uniaxial Tension Test Data for A206 Aluminum

**Table 1:** A206 General Parameters Extracted from Uniaxial Tensile Curve

A206-T6 Aluminum	
<b>Elastic Modulus, GPa</b>	65.392
<b>Yield Strength @ 0.2% Offset, MPa</b>	248.3
<b>Ultimate Tensile Strength, MPa</b>	370.5
<b>Elongation @ Failure, %</b>	9.03
<b>Density, g/ccm</b>	2.796
<b>Poisson's Ratio</b>	0.33

Within FEA solvers, the plastic curve portion of this elastoplastic material data can be created using multiple methods. The method used in this report is the Johnson-Cook curve fit method. This follows the following equation format:

$$\sigma = [A + B(\epsilon_p)^n][1 + C * \ln(\dot{\epsilon}_p^*)][1 - (T^*)^m] \quad \text{Eqn. 1}$$

Where  $\sigma$  is the stress, A is the yield stress, B is the strain hardening coefficient, n is the strain hardening exponent, C is the strain-rate coefficient,  $\dot{\epsilon}_p^*$  is the normalized plastic strain rate defined in equation 2,  $T^*$  is the normalized temperature defined in equation 3, and m is the temperature softening exponent.

$$\dot{\epsilon}_p^* \equiv \frac{\dot{\epsilon}_p}{\dot{\epsilon}_{p0}} \quad \text{Eqn. 2}$$

Where  $\dot{\epsilon}_p$  is the input strain rate (strain rate at any given time), and  $\dot{\epsilon}_{p0}$  is the reference strain rate of the stress-strain data.

$$T^* \equiv \frac{T - T_0}{T_m - T_0} \quad \text{Eqn. 3}$$

Where T is the current temperature,  $T_0$  is the reference temperature, and  $T_m$  is the melting temperature of the material.

The Johnson-Cook curve is a version of von Mises plasticity which assumes isotropic hardening and can account for both strain rate and temperature effects on the material. [11] Note that the isotropic hardening assumption is critical in this model and in future modeling of the CNG tank.

Isotropic hardening assumes that the plastic properties of a material are the same in tension and compression even after plastic deformation occurs. Therefore any work hardening done in a tensile element will increase its compression properties equally. In models, this hardening approach is considered valid when there is no cyclic loading that alternates compression and tension.

For completeness, and to help potential cyclic loading models, the alternative hardening approach is called kinematic hardening. This model assumes the yield surface shifts as the material yields in compression or tension. Therefore, yielding in compression will cause a decrease in required stress to yield in tension and vice versa.

The Johnson-Cook parameters for the A206 aluminum can be found in Table 2. The units for these parameters match the units used in the simulations (kg, mm, ms).

**Table 2:** Johnson-Cook Material Parameters Fitted to Tensile Test Data

Johnson-Cook Parameters for A206 Aluminum	
A – Yield Stress, GPa	0.2483
B – Strain Hardening Coeff, GPa	0.4156
n – Strain Hardening Exponent	0.4908
C – Strain-Rate Coeff, GPa	0*
m – Temp Softening Exponent	n/a*

These values were found using an optimizer utilizing a Davidson-Fletcher-Powell (DFP) algorithm with a golden section internal optimizer once the search direction was found. The optimizer minimized the mean square error (MSE) between the Johnson-Cook curve and the tensile data points. This method was used because the excel curve fit function was not approximating the elastoplastic region of the data properly at the time. Note that the optimizer only handled 2 variables (B and n); the A parameter is known to be the yield strength. As such, which optimizer is used is not critical – this optimization can also be done manually using many iterations. The C parameter was tested on a split Hopkinson bar at Michigan Technological University at various strain rates and found to be approximately zero. Similarly, the m parameter is considered to be not applicable because  $T^*$  is 0 for our simulations (performed at ambient temperature from the NGV2 test standard).

### 3.4. Concrete Material Model

The concrete material model only applies for impact analysis and uses Portland cement concrete, a common, general purpose concrete. [12]

An elastic material model was selected to model this concrete – this assumes the concrete does not fail by plastic deformation or fracture. Since concrete is typically brittle, the ‘no plastic deformation’ assumption should be valid. The ‘no fracture’ assumption is only valid if the concrete is not reaching stresses high above its ultimate strength. By assuming an elastic model without fracture for the concrete, the concrete no longer has an energy release mechanism; the stored energy must therefore stiffen the structure and increase the reaction forces on the tank. In effect, the elastic concrete will stiffen where actual concrete would release energy via fracture therefore creating a ‘worst-case’ scenario for the tank. The associated concrete properties are given in Table 3.

**Table 3:** Concrete Elastic Properties for Portland cement concrete [12]

Portland Concrete Elastic Properties	
Elastic Modulus, GPa	13.789
Density, g/ccm	2.24
Poisson's Ratio	0.2

In future, fracture characteristics may need to be considered to ensure an accurate model. This should be used only if physical testing shows a large discrepancy in strains when compared to simulations.

## 4. Mesh Selection

Of the 3 general options for elements (1d, 2d shell and 3d solid), only 2d and 3d element types are considered for this report. While 1d elements have potential to approximate internal geometry, the error is likely to be too large to make it worth the run-time reduction. As such, they are considered a potential area for future model reduction.

### 4.1. Shell v. Solid Elements (First Order)

2d elements are typically used in thin structures with small to no thickness gradients. Compared to 3d elements they reduce run time and avoid problems such as shear locking. The two primary element types are quad (4 side) and tria (3 side). Quads are typically preferred since trias demonstrate difficulty in modeling bending problems. Both types may be subject to hourglassing.

The internal geometry of the tank fits the requirements for a 2d mesh; there are no thickness gradients or complex interfaces. However, the 3-radius interface shown in Figure 7 and external geometry limit potential uses for 2d elements. A 2d mesh of the 3-radius interface misses the connectivity between surfaces caused by the radii and the external geometry has thickness gradients close to these interfaces. Therefore, a 2d mesh is not recommended for the entire tank.

3d elements are the default element for 3d structures. The two primary elements are hex (6 side cuboid), tetra (4 side triangular prism) and the connector pyramid element (5 side pyramid). Hex elements are preferable as they shear lock less than tetra and pyramid elements. Pyramid elements are only used when a transition between hex and tetra elements is needed.

While hex elements are preferable, the tank geometry does not allow for parallel quad meshes to create a valid set of hex elements. Therefore, a tetra mesh is the recommended

3d element style to model the tank if only 1 element type is used. These elements are used for all initial convergence testing and defining baseline model results.

## 5. Static Modeling – Starting Mesh Size Determination

Initial modeling with static analyses is used to reduce the number of simulations required to test convergence in the dynamic analyses. As such, the static convergence models cover a large set of element sizes and assess potential variability in resultant stresses to find a converged element size. The chosen range for element sizes is from 2.5mm to 5mm by 0.5mm increments. The maximum element size was chosen because the mesh begins to have 1 solid element through the tank thickness at this size. This violates the general rule for 1<sup>st</sup> order 3d meshing; always have a minimum of 2 elements through the part thickness. The minimum size was chosen as an estimate of the minimum size desired in impact analysis to maintain a reasonable runtime.

### 5.1. Static Model Overview – Boundary Conditions

#### 5.1.1. Static Displacement Constraints

The CNG tank shown in Figure 6 in the *Tank Geometry* section is a full phase 1 tank. However, since the tank is symmetric and internal pressure is uniform, the tank model for static pressure can be cut along each plane of symmetry as shown in Figure 10.

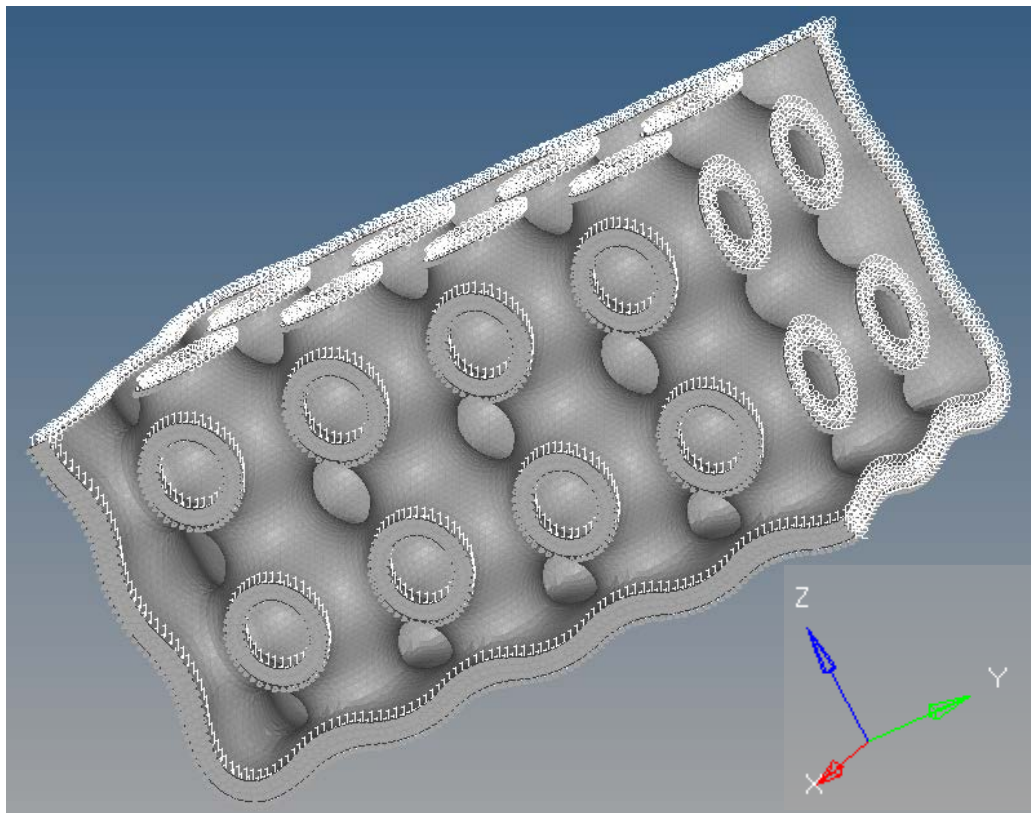


**Figure 10:** Symmetry Boundary Conditions in Static Pressure Analysis

Along each of the 3 planes of symmetry, boundary conditions are set constraining translation in the normal direction of that plane (ex. x-y plane of symmetry is constrained in the z-direction). These constraints match the actual displacement of a full pressured tank since the mid-plane of a symmetrically loaded specimen will not move.

### 5.1.2. Static Loading Conditions

The load conditions for static analysis match those of a tank at operating pressure of 3600 psi as shown in Figure 11.

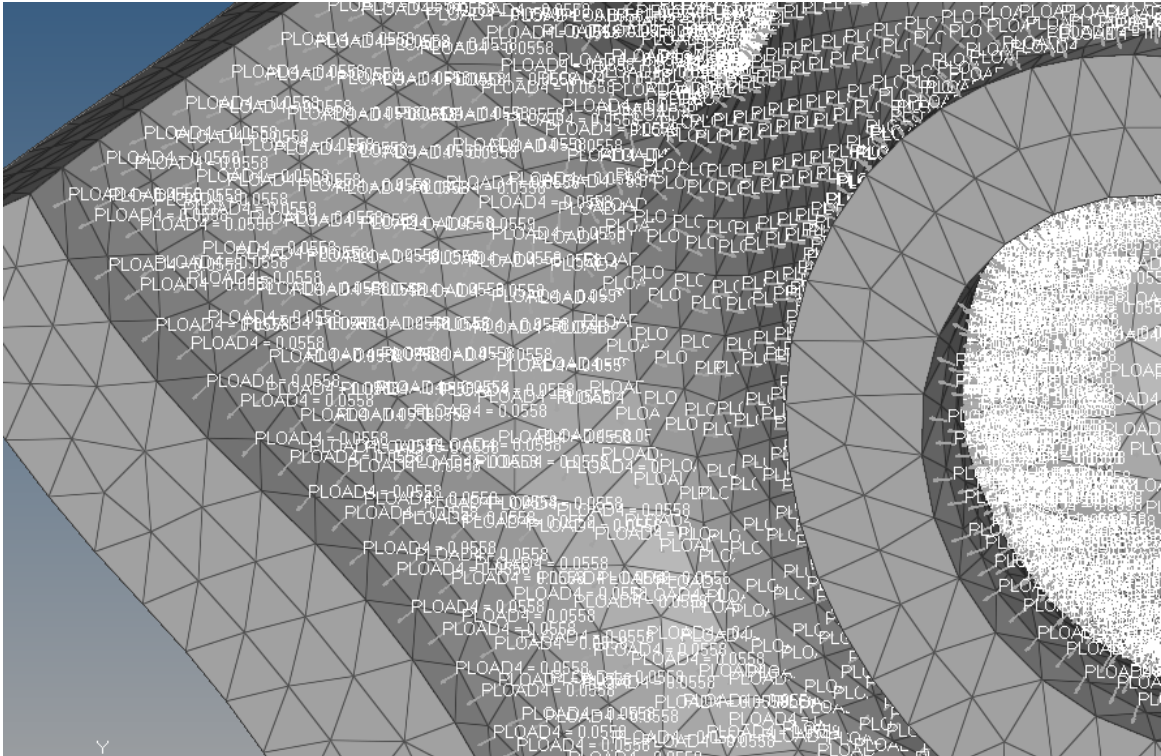


**Figure 11:** 3600 psi Pressure Loading Conditions on Phase 1 Quarter Tank

While this pressure could have been set to 8100psi, the convergence study was performed at 3600psi to compare with and validate convergence study data from previous students. However, since the load conditions would not change beyond a simple scalar multiplier the convergence of a 3600psi load should match that of an 8100psi load.

### 5.2. Static Convergence Criteria

Since this convergence study was initially performed before knowing more about convergence, the criteria used to define convergence was the maximum von Mises stress (75% average). Note that a 75% average (known as simple average in HyperView) is used to reduce the effect of stress gradients within the tetra elements. Therefore, while metrics such as recoverable strain energy are now known to be more useful, the issues



associated with element stress gradients in using maximum non-averaged stresses as the convergence criterion should be minimized.

In an effort to further prove convergence with standard deviations, 3 simulations were run at each element size. In each simulation the model was created using a building block mesh. This mesh formed the entire tank by creating a 2-by-2 set of cores and extending it either in the x, y or z direction. Each of the 3 simulations had a different primary extension direction. This method forces all element quality criteria to be identical within an element size setting and therefore removes noise associated with remeshed element quality. The only variable tested by this standard deviation is what element stacking orientation effects are on the model. Therefore, the standard deviation for these models can be considered a true standard deviation used to determine whether models are equivalent or not. A supporting visual for this method is shown in Figure 12.

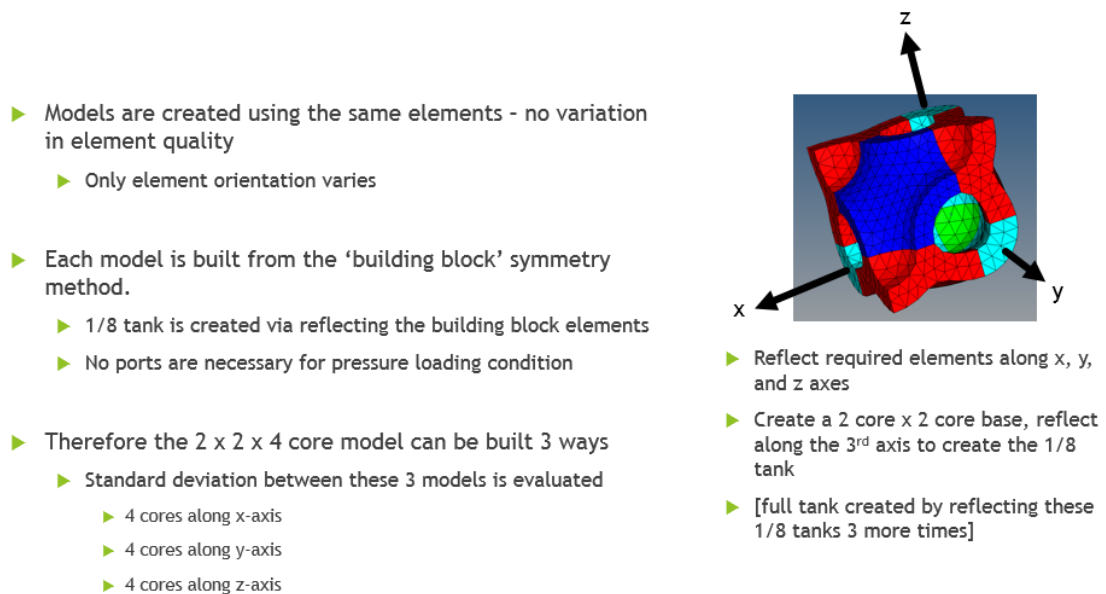


**Figure 12:** Method to Assess Standard Deviation in Symmetrically Formed Tank

### 5.3. Static Analysis Results

A sample set of stress results from the simulation are shown in Figure 13.



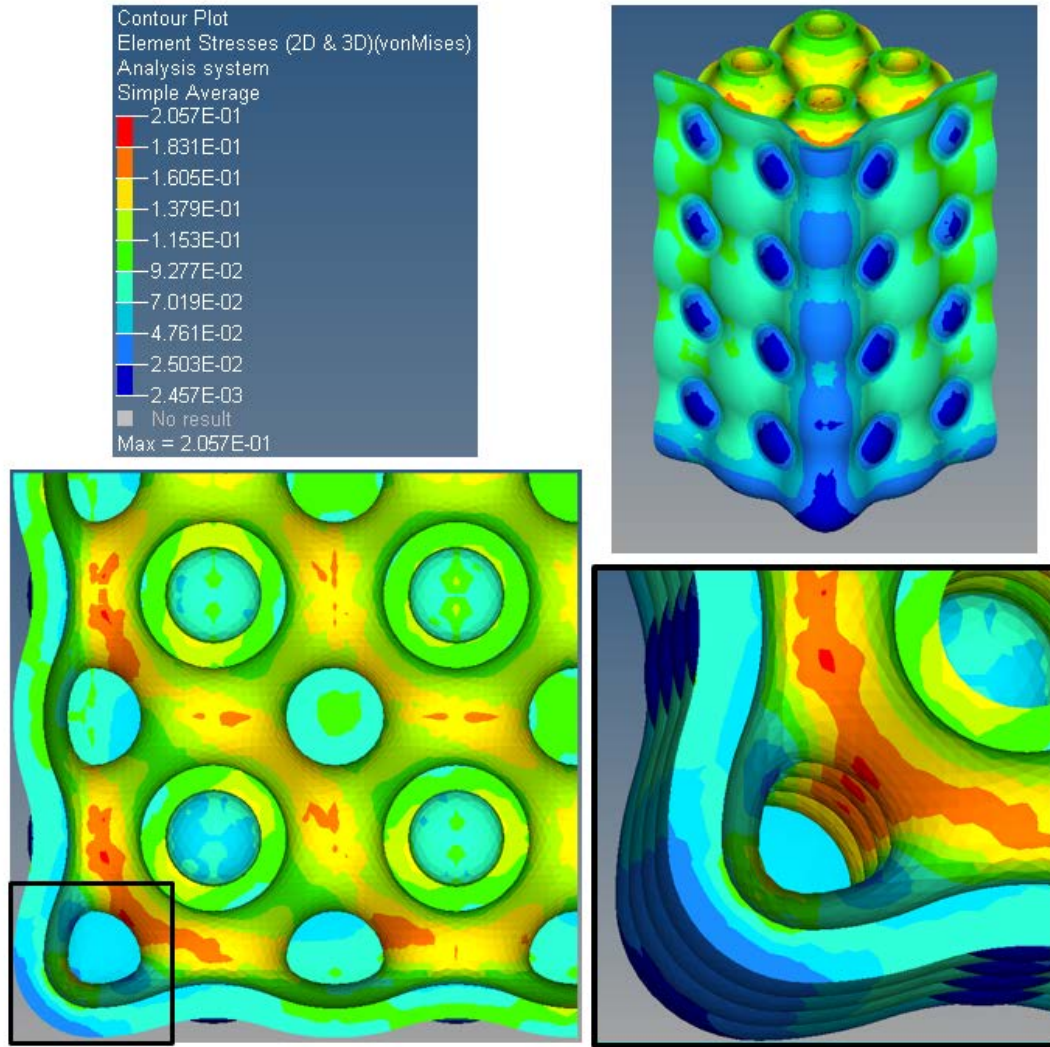


**Figure 13:** 3mm z-extension Static Test Results at 3600 psi: Simple Average Mises Stress

Note that the stress results are given in GPa due to the simulation units used. The maximum stress in this simulation is therefore 205.7 MPa. These images show the location of maximum 75% averaged von Mises stress in the model; this location is consistent between models and is a key defining feature of the static analysis for all pressures.

Another defining feature of the model is that the stress is not completely symmetrical along the 2x2 section of the model (shown in the bottom left image). This demonstrates the rationale for measuring the standard deviation of the models that occurs from mesh stack-up error. If there are small differences using identical elements, the impact of orientation should be considered.

Convergence results for the CNG tank including standard deviation are shown in Table 4 and Figure 14 respectively.

**Table 4:** von Mises Stress and Standard Deviation at Various Element Sizes with 3600 psi Loading

Element Size, mm	Average Max von Mises Stress (% Error), MPa	Max von Mises Stress Standard Deviation (%Error), MPa
2.5	215 (0)	3.2 (1.5)
3	206.3 (4)	4.9 (2.3)
3.5	201.5 (6.3)	2.3 (1.1)
4	193.2 (10.1)	1.1 (0.5)
4.5	172.9 (19.6)	6 (2.8)
5	167.3 (22.2)	3.5 (1.6)

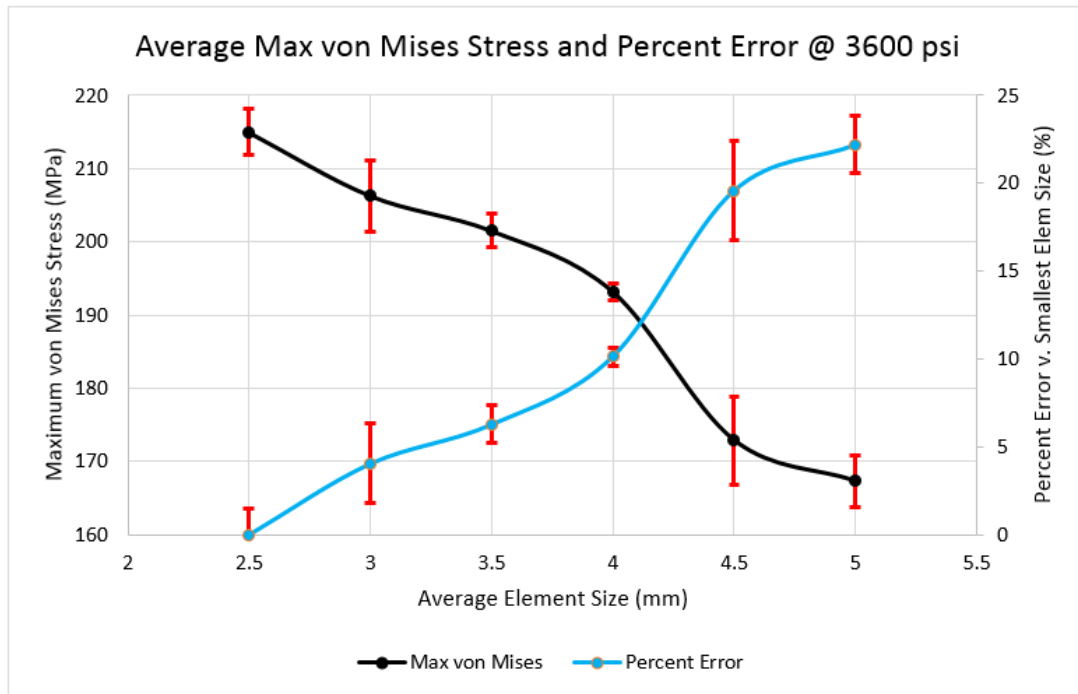


**Figure 14:** Average Maximum von Mises Stress v. Element Size at 3600 psi with Error Bars

The stress results show a decrease in accuracy below 3.5mm mesh size and a steep drop off in accuracy below 4mm mesh size. Similarly, at 2.5mm there is an increase in maximum stress implying that there is still room to reduce the mesh size to increase accuracy. However, when considering the standard deviation of the model, the 3mm mesh size should be considered acceptable compared to the 2.5mm mesh size. Therefore, the 3mm mesh size is chosen as the starting element size for dynamic impact analysis.

The standard deviation of these convergence results demonstrate the difficulties with convergence criteria. While convergence can still be estimated, there is up to 2.8% error in noise associated with mesh orientation in this model. When compounded with other noise factors such as remeshed elements (varying element quality), and numerical error in the solver this variation may reach 5% or higher. For this report the von Mises acceptable deviation is considered to be below ~5%. This assumes variation will increase due to remeshed elements and considers a statistical 5% error interval – ‘less than 5% error is ‘insignificant’.

## **6. Dynamic Modeling – Convergence Verification**

While dynamic modeling of convergence takes longer, it is necessary to understand convergence of the impact load condition. Since convergence of a model is defined by having a small enough element size to accurately calculate the deformation tensor (and by extension the stress, strain etc.), a significant change in load conditions implies a potential change in converged element size. However, instead of using a large range of element sizes, we can test a smaller range for convergence based on the convergence estimated in the *Static Modeling* section. Due to the higher stress concentrations of the load conditions it is safe to assume that the converged element size should not be larger than the converged range of static analyses. Therefore, the selected element size range was chosen to include 2.25, 2.5, 3, 3.5 and 4mm mesh sizes. No standard deviation was considered for these models.

Within these element sizes a modified edge drop test condition was the primary focus. The edge (45° rotation) drop test will have larger stress concentrations than the horizontal drop test because the contact surface is smaller. In order to ensure this is the case for any CNG tank, the drop height was changed to be 72” from the lowest point of the tank. This test condition matches that of the horizontal drop test. Therefore, the converged element size from these results can be used for any test condition.

In addition to an edge drop test, convergence was analyzed for a corner drop test (45° / 45° rotation). This test condition is a worst-case scenario for stresses applied to the tank. Therefore, convergence results will provide a second estimate of the minimum element size required for convergence.

## 6.1. Dynamic Model Overview – Boundary Conditions

### 6.1.1. Dynamic Displacement Constraints

Displacement conditions for the drop test are set on the concrete block on all outer surfaces except for the impact surface as shown in the sketch and actual model views of Figure 15.

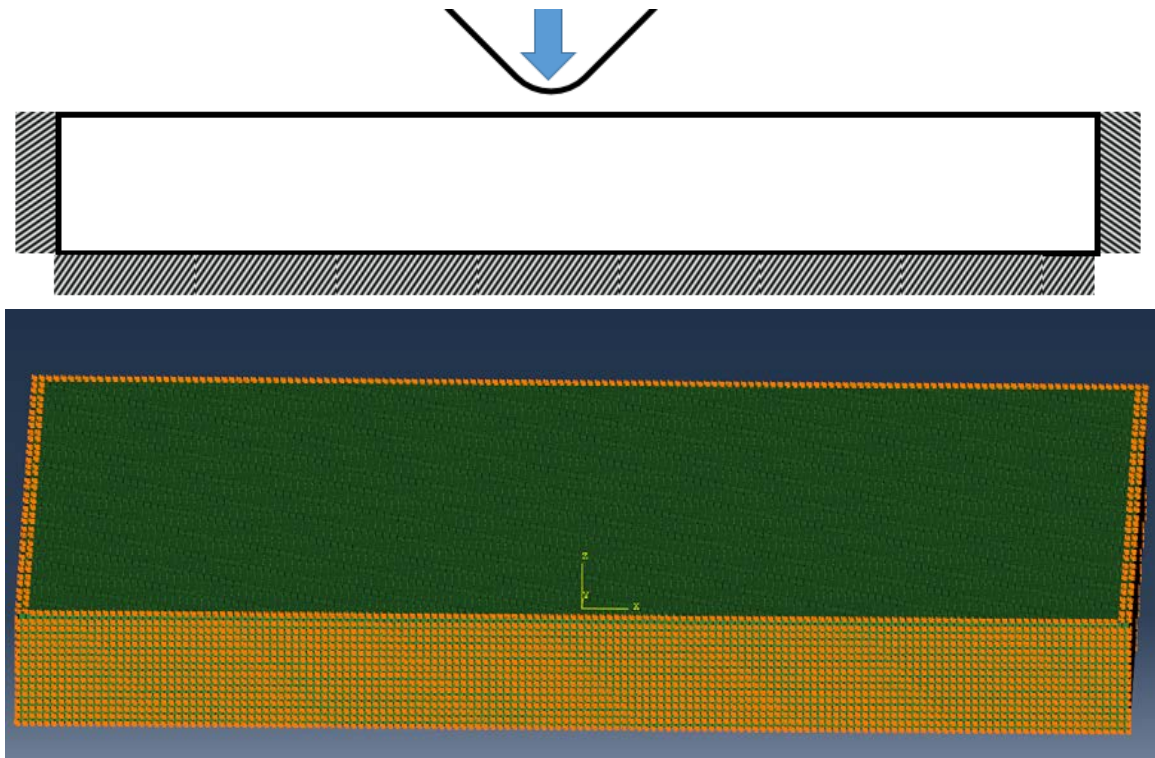


**Figure 15:** Sketch of Constrained Concrete Slab (top) and Model of Constrained Slab (bottom)

This configuration assumes that the sides and bottom surface of the concrete are not allowed to move during impact. This ‘no bending’ assumption was chosen as a worst case scenario; minimizing bending in an elastic model increases the concrete contact forces resisting deformation during the impact.

The alternate assumption is to leave the bottom of the concrete unconstrained (similar to conditions where it may bend slightly, such as compressing dirt below the concrete). Since dynamic simulations show minimal deformation of the concrete, the difference between the two assumptions should be minimal. The worst case scenario with no bending is preferable for determining convergence.

### 6.1.2. Dynamic Loading Conditions

Loading conditions are applied to the tank such that the kinetic energy from a 72" drop is converted to an initial velocity. The kinetic energy of each run is calculated to be approximately 742.3 J. This initial velocity is derived from the mass of the tank (~41.24 kg) and the transfer of 100% potential energy of the tank at 72" to 100% kinetic energy of the tank at 0". Using this mass, the initial velocity is approximately 6 m/s for the baseline 3mm phase 1 tank as shown in Figure 16 via sketch and model images.

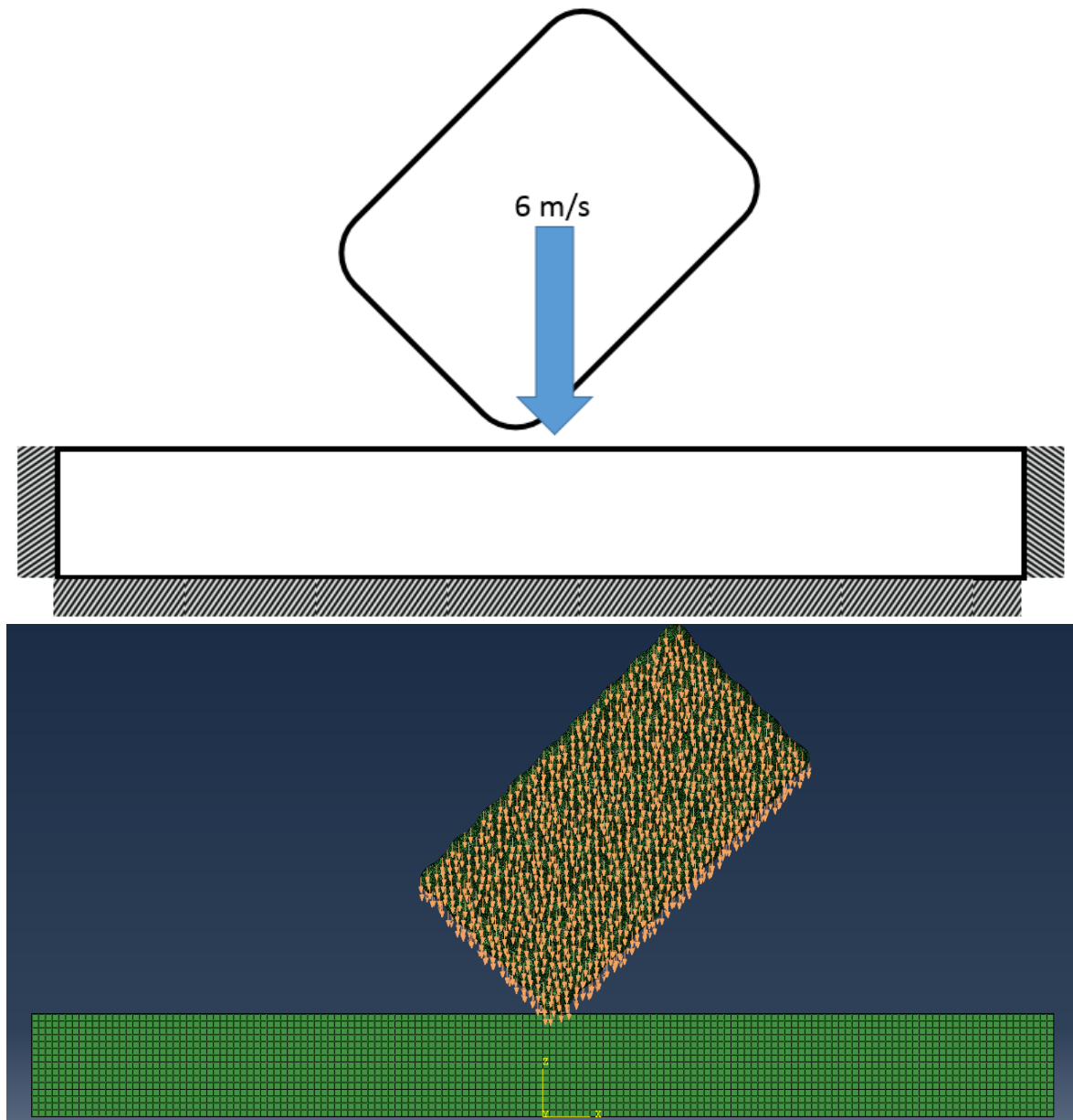


**Figure 16:** Sketch of Initial Velocity Condition (top) and Modeled Velocity Condition (bottom)

It is critical to note that the mass of the tank will have small fluctuations depending on the mesh size. This occurs due to geometric approximation of elements adding or subtracting small amounts of mass. Therefore the tank velocity is recalculated for each model using 742.3 J as the target initial total energy.

### **6.1.3. Dynamic Contact Controls**

This impact analysis considers contact to be a frictionless kinetic contact. The frictionless assumption is typically considered valid in small-deformation systems. Friction in the model serves to increase the shear force on the contact elements. With small deformation, the contact surface is minimal and shear forces will be a small component in the analysis. Because of this, as long as the friction setting is consistent it will not affect convergence results. Friction may need to be considered in future models to ensure model accuracy compared to physical testing.

The kinetic contact method uses a predictor/corrector algorithm. It is designed for precise enforcement of contact conditions and is recommended for contact with elastic materials (such as the concrete slab). Since the driver for loading in the simulation is contact, this style of contact control is preferable. Limitations of this contact method include: inability to model rigid-rigid contact, cases with ‘chatter’ contact (vibrations) and has difficulties when interacting with other constraints (typically one constraint is removed if interference occurs).

For completeness, the alternate method is the penalty contact method (via penalty algorithms). This method is considered the ‘general’ contact method and can account for more types of contact (such as rigid-rigid contact) and interacts well with other constraints, but will introduce minor additional stiffness as the contact is “less stringent” in enforcing the constraint (penalizing any penetration so the solver can correct it via reaction force). The primary limitation of the penalty method contact analysis is any large deformation at the contact surface with high reaction forces. These scenarios may be caused by displacement-controlled loading, coarse mesh, or elastic responses where large deformation occurs. Additionally, Abaqus estimates this method to decrease the timestep by up to ~4%. [13] Since many of these conditions are met and the timestep decrease is not ideal, this method is not chosen in this simulation.

## **6.2. Dynamic Convergence Criteria**

There are 3 different convergence criteria considered for these models: Recoverable strain energy (strain energy), internal energy (total strain energy), and average maximum signed von Mises stress (75% average). Each criterion is only considered for the tank, not the entire model (tank and slab).

Internal energy, in reference to this simulation, is defined as the sum of elastic and plastic strain energy of the tank. As such it is more sensitive to stress gradients within elements and can vary accordingly. Recoverable strain energy is only the elastic strain energy of the tank; while this criteria is less inclusive than internal energy, it is more robust as a



convergence criteria in elastoplastic models as high stress gradients will not contribute to the recoverable strain energy. The simple average signed von Mises stress is also measured because it is the primary output considered in the models and has a clear physical connection to the results. As such this measure should still be included when assessing a converged model. In physical validation this criteria should also include strain.

For completeness it must be noted that signed von Mises stress (as opposed to regular von Mises stress) is the desired metric to track for failure criteria in the drop test simulations. Signed von Mises stress looks at the sign of the first principal stress in an element and gives the same sign to the corresponding von Mises stress. This is critical for this model because the edge/corner is put into bending. This bending applies a larger compressive stress than tensile stress to the material. Since aluminum fails at different compressive and tensile stresses and the compressive strength is known to be much higher than the tensile strength due to plastic flow, we focus on tensile stresses in the model.

### 6.3. Dynamic Analysis Results

A sample set of von Mises stress results from the simulation are shown in Figure 17.

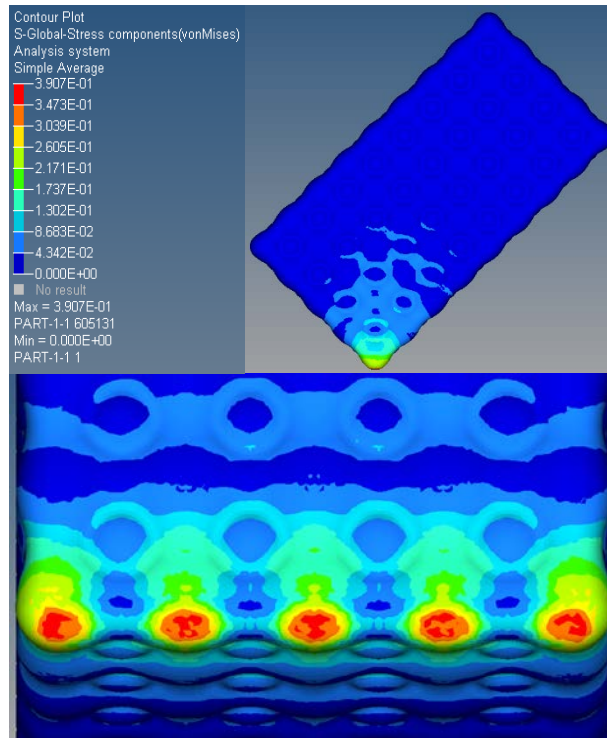


**Figure 17:** von Mises Stress Results for 2.25mm Element Size with Maximum Stress Region (bottom)

Note that the stress results are given in GPa due to the simulation units used. The maximum stress in this simulation is therefore 390.7 MPa. These images also show the location of maximum 75% averaged von Mises stress in the model; this location is consistent between models.

While the model shows minimal deformation, it is important to note there is not symmetry of the stresses along the tank in these runs. This is because the tank is not located along the midplane of the concrete slab. This does not affect the convergence results but must be recognized in future modeling efforts. The reason for this effect is because the concrete can deform less near the boundary conditions. Therefore, the contact forces closer to the edge of the slab are slightly larger.

Another key feature to note is that the maximum stress exceeds the tested ultimate strength of the material. The Johnson-Cook material model does not have an input maximum stress. This allows the stress to continue along the estimated stress-strain curve which avoids any truncation past the ultimate tensile strength. Additionally, as mentioned in the *Dynamic Convergence Criteria* section, the signed von Mises stress is a better measure of failure in this model. The maximum stress regions shown are compressive regions, while the stresses on the inside of the tank are in tension. Because of the geometry, the internal stresses are much lower than the external stresses. The von Mises stress results shown in Figure 17 are shown in Figure 18 in signed von Mises stress for comparison.

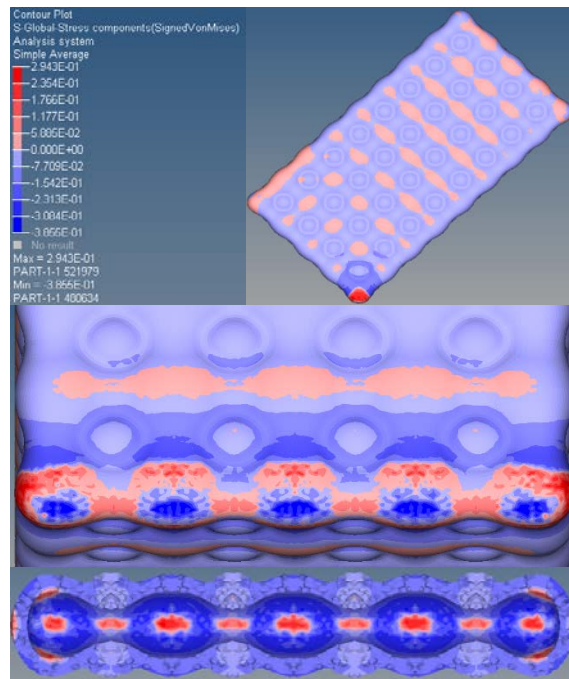


**Figure 18:** Signed von Mises Stress Results for 2.25mm Element Size with Maximum Compressive Stress Region (middle) and Maximum Tensile Region (bottom)



The previous maximum von Mises stresses are shown to be compressive stresses while the new maximum tensile stress is located on the inside of the tank as shown in the bottom image of Figure 18. However, by using signed von Mises stress in regions where the stresses alternate between tensile and compressive, the stress gradients appear to be larger than that of regular von Mises stress. This occurs due to averaging.

Convergence results for the CNG corner tank impact are shown in Table 5 and Figure 19 respectively. Similarly, convergence results for edge impact are shown in Table 6 and Figure 20 respectively.

**Table 5:** Convergence Criteria and Run Time at Various Element Sizes in Drop Test

Element Size (mm)	Average Max Signed von Mises Stress (%Error), MPa	Recoverable Strain Energy (%Error), MPa	Internal Energy (%Error), MPa	CPU Run Time (%Change), hr:min
4	279.3 (4.7)	83.3 (20)	413.3 (2.6)	1:02 (90.5)
3.5	282.8 (3.5)	76.0 (9.6)	417.7 (1.6)	1:50 (83.3)
3	291.5 (0.5)	72.0 (3.8)	419.7 (1.1)	3:10 (71)
2.5	293.4 (0.1)	70.5 (1.7)	423.20 (0.3)	7:06 (35.2)
2.25	293.0 (0)	69.3 (0)	424.29 (0)	10:58 (0)

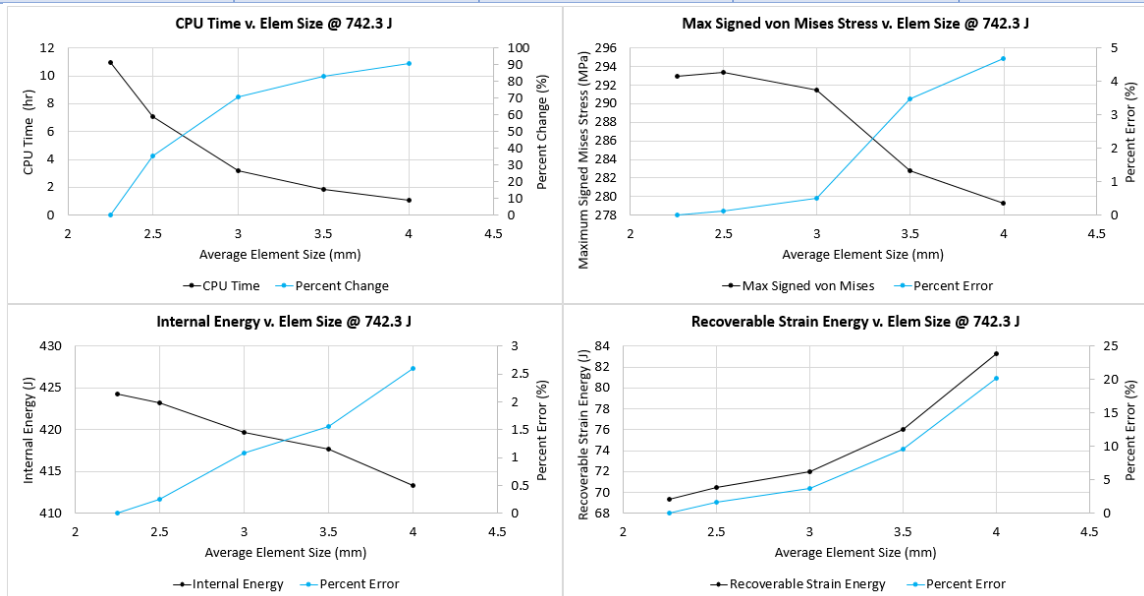


**Figure 19:** Graphed Convergence Criteria and Run Time v. Element Size for Corner Drop Test at Constant Initial Kinetic Energy (742.3 J)

**Table 6:** Convergence Criteria and Run Time at Various Element Sizes in Edge Drop

Element Size (mm)	Average Max Signed von Mises Stress (%Error), MPa	Recoverable Strain Energy (%Error), MPa	Internal Energy (%Error), MPa	CPU Run Time (%Change), hr:min
4	245.3 (16.6)	153.2 (5.4)	463.9 (1.9)	1:00 (90.6)
3.5	247.8 (15.8)	151.0 (3.9)	469.2 (0.8)	1:50 (82.6)
3	259.9 (11.7)	152.5 (4.9)	467.5 (1.2)	3:03 (71.2)
2.5	293.6 (0.2)	146.9 (1)	475.3 (0.5)	6:34 (38.2)
2.25	294.3 (0)	145.3 (0)	473.1 (0)	10:37 (0)

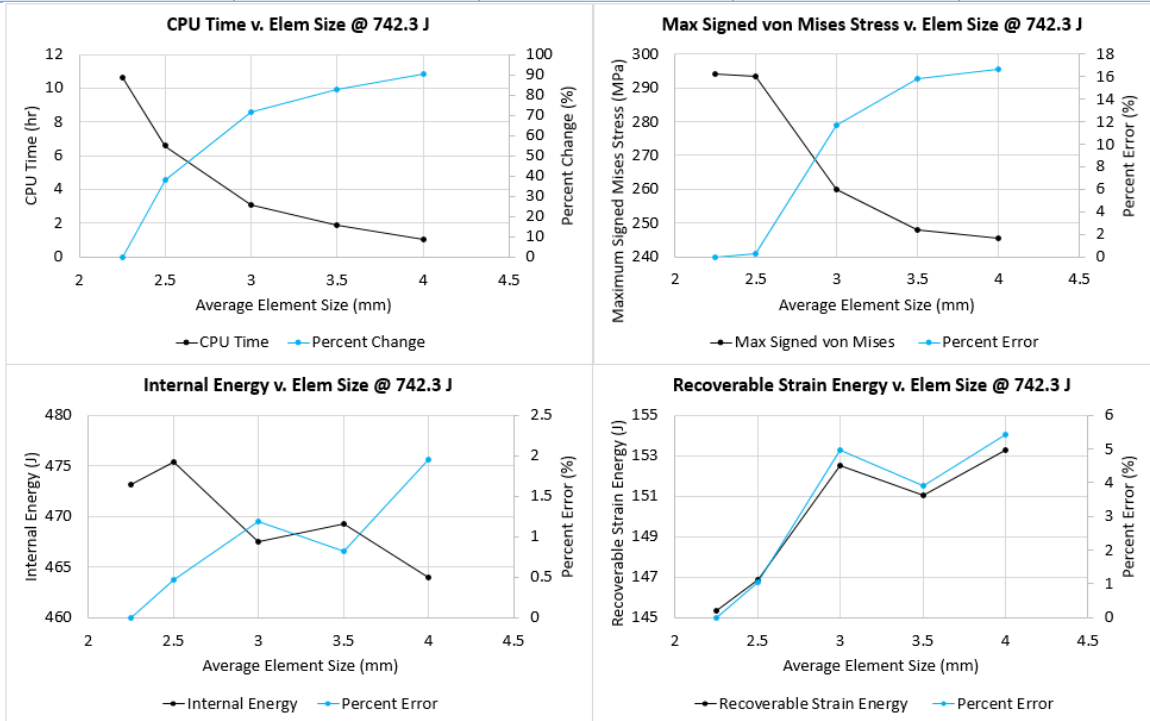


**Figure 20:** Graphed Convergence Criteria and Run Time v. Element Size for Edge Drop Test at Constant Initial Kinetic Energy (742.3 J)

Assuming an acceptable convergence of 5% or less, the stress and energy results indicate a minimum element size of 3mm for the corner impact. The edge impact results imply an element size of 2.5mm. This discrepancy is likely due to the ‘simple’ nature of the corner impact where there is only 1 impact location. In the edge case, 4 different contact points impact the concrete with varying concrete stiffness at each point due to the boundary conditions. This results in more simulation noise. The edge impact case can therefore be

considered a more complex impact scenario and the driver for convergence if a non-infinite concrete block is used.

From the stress results, it can be concluded that the models are either converged or beginning to converge at 2.5mm. The corner and edge impact percent difference between stresses from 2.5 to 2.25mm are both below 1%.

Contrary to this, the energy results seem to be continuing to increase / decrease instead of completely tapering off at 2.25mm element size. This may indicate that the model is still not 100% converged at 2.25mm. The energy results therefore support the static analysis results that the convergence can be improved further. However, because the model already requires 10.5 hours to run at a 2.25mm element size and because runtime displays an exponential growth as element size decreases, this element size is considered the minimum allowable size for the scope of this paper (and is recommended to be considered a minimum for optimization purposes).

With this assumption, the 2.5mm element size can be considered a valid converged element size as there is minimal difference in output stress and only minor error in energy results between these element sizes. While this assumption will introduce error, it should not affect the results of applying time reduction methods to the model. As long as the time reduction methods are applied at a constant element size, noise associated with convergence will be minimized.

For energy convergence criteria, it is critical to note that the difference between runs is on the order of 1's in Joules. Considering this is very small compared to the actual value (less than 5% error in all cases of internal energy), it is difficult to decide upon a useful percentage error that may be acceptable. This is reinforced by the fact that strain energy (and strain energy density) are calculated over a specific area. In this case the entire tank was used, but in cases that only take a small area of the tank, percentage error may fluctuate. Numerical error within the solver may also be the source of this gap as truncation can easily cause error on the order of 1's. Therefore, numerical error should be kept in mind for all convergence results. Additionally it is recommended to include stress in future convergence criteria to maintain an understanding of the physical meaning of error between runs. In physical testing this may also include strain convergence.

## **6.4. Physical Validation**

This section is included for completeness in future modeling of the CNG tank.

Physical validation for drop testing has not been fully carried out at this point. As such, the data that we currently have for impact scenarios is limited to photos as shown in Figure 21.



**Figure 21:** 2.25mm Edge Impact Plastic Maximum Principal Strain Results

Both test scenarios show minimal deformation. A set of comparative views from simulations are shown in Figures 22 and 23.

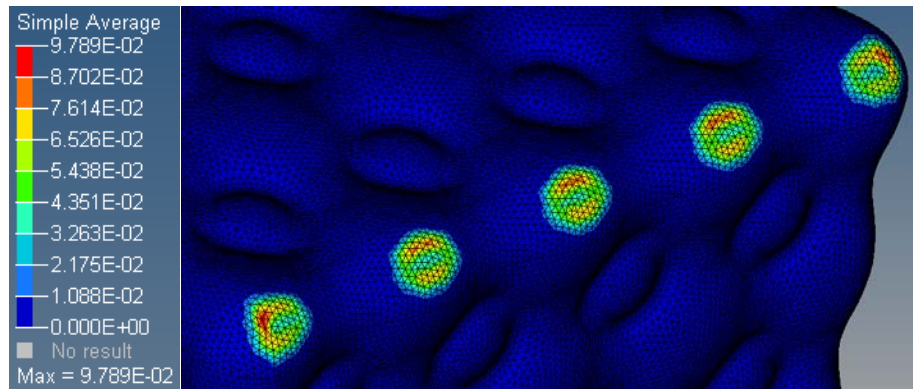


**Figure 22:** 2.25mm Edge Impact Plastic Maximum Principal Strain Results

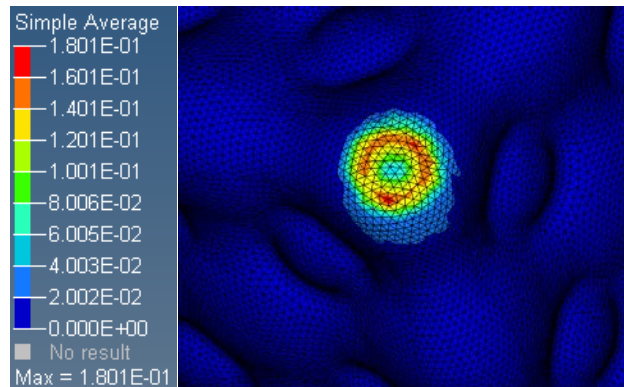


**Figure 23:** 2.25mm Corner Impact Plastic Maximum Principal Strain Results

Note that the deformation of these simulations is ~1.6mm for the edge impact model and ~3.9mm for the corner impact model. Comparing the images, the edge impact case should be considered reasonable for impact conditions. The maximum principal strain is around the maximum seen in the material model and therefore requires minimal extrapolation. Therefore, any errors that occur in measuring deformation are due to gaps in the tensile v. compressive properties of the material.

In the corner impact case, the deformations are larger than depicted in the image. This can be explained by the maximum principal strain which reaches 18% (~2x the maximum tensile strain). This large strain forces the solver to extrapolate the stress-strain tensile curve. Not only does this material curve need to be compressive for a better measure of strain, the approximating tensile curve is significantly extrapolated which is likely the root cause of this error.

Therefore, when further physical tests are performed, strain measurement is highly recommended to improve calibration of the material model. Further compressive material properties may also be necessary to better understand changes in tensile v. compressive properties in the material curve. The simulations should use these results to edit the material model and account for high compressive stress regions. This should improve accuracy of corner impact deformation estimation on the outer surface.

Run time reduction is determined by increasing timestep (function of only element size in these simulations) and decreasing the number of equations to solve (number of nodes). Therefore, alterations to A206 material properties is considered a negligible factor in run time reduction method assessment.

## **7. Time Reduction Methods**

In previous analyses the element size and type was constant throughout the model to ensure a consistent converged element size. However, elements that are located far from the points of contact have minimal stresses and therefore have minimal contribution to the output. Multiple methods can be applied to take advantage of this to reduce run time. Four methods are considered in this paper: a symmetrical ‘building block method’, gradient meshing, hybrid element meshing and planes of symmetry.

There are two additional methods that were considered but not used for run-time reduction in this report. Either the user can opt to use second-order elements and reduce the total number of elements or the concrete floor can be replaced with a rigid wall. These methods are also described with reasoning as to why they were not used.

### **7.1. Symmetrical Building Block**

The symmetrical building block method asserts symmetry in the model. As mentioned in the *Tank Geometry* section, there are a large number of lines in the CAD file that obstruct symmetry in the CNG tank model. However, it is known that the CNG tank is actually symmetric. Instead of toggling each line on each cell (which still misses some geometry

fixes that need to happen), the user can split the model into unique parts. Each unique part geometry is then corrected. The tank model can then be built using these parts (either pre-meshed or meshed in a larger piece). The mesh is then reflected to produce repeating element structures. A set of sample parts used for phase 2 CNG tank modeling are shown in Figure 24.

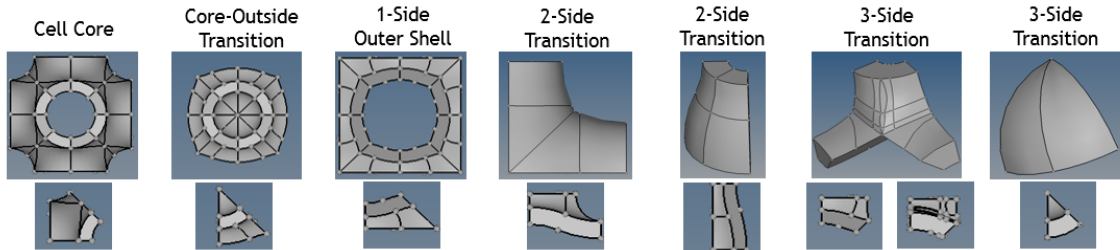


**Figure 24:** Phase 1 and 2 Model – Unique Parts for Conformable Model Creation

Note that the top line shows the bulk piece within the model, and the bottom line shows the piece the user needs to mesh. These small pieces represent the entire geometry of a Phase 1 or Phase 2 tank (assuming only 90° corners and edges occur). In all cases, the smaller blocks can be merged and meshed to form a larger component to be reflected like the one shown in Figure 25.

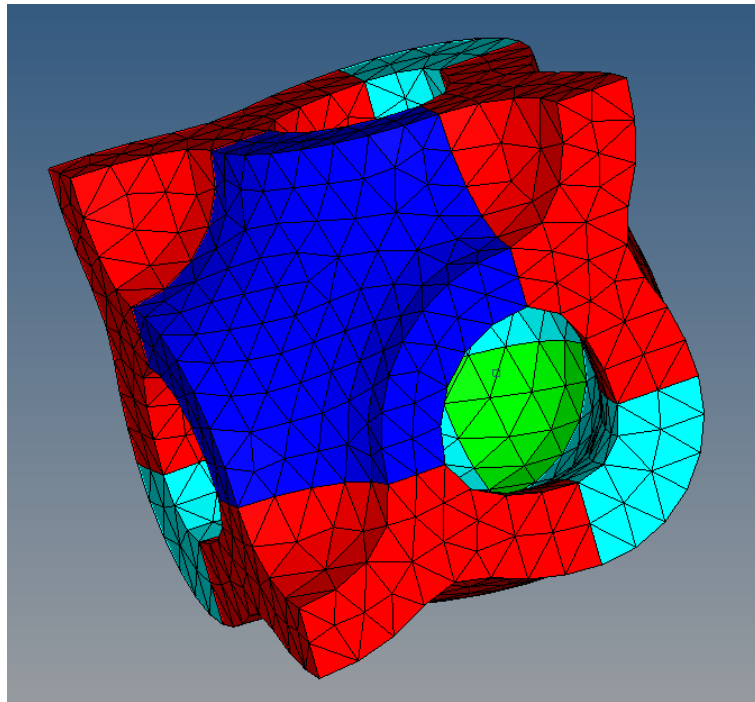


**Figure 25:** 4mm Phase 1 Base Part – Colored Segments Indicate Different Parts from Figure 20

The CNG tank model can be formed from this part simply by reflecting segments of the base part. Each reflection follows geometric lines created by boundaries between parts. This method is ideal to enforce a defined element size and element quality in the model and ensures that stress concentrations do not occur in local regions due to differing mesh quality. Additionally, once the parts are created, various tank geometries can be quickly formed by rotating and reflecting these components. Therefore this method also reflects a decrease in model creation time for all models after the building blocks are created.

## **7.2. Gradient Meshing**

Gradient meshing is a common approach in FEA simulations where areas of minimal impact are meshed at a larger element size than the critical zones. In effect, a gradient is formed with small (converged) elements at the critical locations going to a larger element size far away from these locations.

This method should be used for any model that has areas with minimal impact. However, it is important to note the limitations to this gradient. Because there are elements that transition from small to large element sizes, the transition should maintain the element quality required of all other elements (typically the aspect ratio and jacobian are worse in transition regions). To this point, the user must ensure that the gradient does not significantly change the results of the simulation. In the case that they are affected, the transition mesh may need to transition slower or begin farther from the critical location. Determining if the results are significantly changed requires a full model to be tested at the selected element size. While this may not be possible for very small element sizes (ex. 1mm in the dynamic cases), it is the easiest method to prove results are not significantly changed when gradient meshing.

## **7.3. Hybrid Element Meshing**

Hybrid element meshing takes advantage of the fact that lower dimension elements take less time to solve in an FEA solver (3d vs 2d vs 1d). In this paper, the hybrid element meshing method uses a transition between 3d and 2d elements. As mentioned in the *Element Selection* section, 2d elements are not ideal in the external surface and 3-radius interface but are usable for the internal geometry. Therefore a transition region can be set up such that the shell elements connect with the solid elements allowing the external surface and 3-radius interface to be modeled with solid elements and the internal surface to be modeled with shell elements. Figure 26 shows a sample hybrid mesh region.



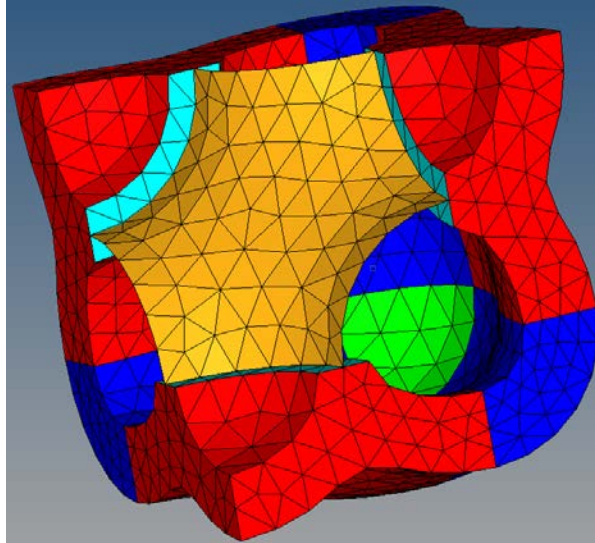


**Figure 26:** Hybrid Element Mesh for 4mm Hybrid Model – Transition Elements in Light Blue

Note that there are shell elements (light blue) covering the surface of the solid elements at the 3-radius interface (red). These elements help transfer bending rotation of the 3d elements to the shell elements on the internal P-surface (orange). Without these elements any rotation of that surface about the point of contact between internal and external surface would not be transferred to the internal surface. Despite this, the hybrid transition will still not properly transfer shear stresses. Therefore, it is recommended to place this transition away from critical regions similar to a gradient mesh.

#### **7.4. Planes of Symmetry**

Depending on the simulation there may be planes of symmetry that can be used to reduce run time. The analyses for the time reduction consider only edge impact which has 1 plane of symmetry. Note that a plane of symmetry requires both the load conditions and geometry to be symmetrical, therefore only 1 plane of symmetry exists while the static load case had 3 planes of symmetry.

This method does not require simulation to understand – in a symmetrical model the run time will be reduced by approximately half for each plane of symmetry (nodes on the plane of symmetry are not halved). Planes of symmetry only change the number of elements (not the timestep) and therefore are linearly related to the run time.

#### **7.5. 2<sup>nd</sup> Order Elements**

Second order elements are typically used to increase accuracy without increasing the number of elements in a model. These elements increase the number of nodes which fixes first order stiffness problems (ex. shear locking or tria bending stiffness). Additionally



these elements will converge at larger element sizes which may allow for lower run times.

The rationale for not using second order elements in this analysis is due to the thickness of the tank. Since the tank is thin, only 1 to 3 elements can fit within the thickness in the range of first order elements tested. Therefore it is difficult to reduce the element size far enough to make the computational time lower than the first order response. Additionally, even if the element size can become large enough, the second order elements will still not match the actual geometry. The element analysis tensors (deformation, strain, stress etc.) may be second order but the element geometry remains first order. Any error associated with geometry mismatch will not be fixed.

## **7.6. Rigid Wall**

Using a rigid wall instead of a meshed concrete floor will save run time. However, this run time is not related to the tank; therefore any percent decrease in run time associated with using a rigid wall will be constant no matter the size of the tank.

Future iterations of the CNG tanks will need to make this decision based upon accuracy v. run time. Using a rigid will reduce time due to removing elements. Additionally, it will reduce noise associated with where the tank is dropped on the cement slab due to a constant stiffness (infinite) at all points.

If the user prioritizes run accuracy, a rigid wall is not recommended. The amount of elastic energy absorbed by the concrete in edge and corner impact was approximately 140 J and 60 J respectively. This increase in energy ranges from 10% to 30% of the energy absorbed by the tank in concrete impact simulations. While drop location on the concrete slab will affect maximum stress, a consistent drop location can fix this issue; the increase in energy however cannot be corrected in the model.

Additionally, because the rigid wall has an infinite stiffness, the relative stiffness of the tank to the rigid wall is very small. This large gap in stiffness will cause truncation error in the analysis responses and potentially add more noise to the simulation results (in addition to error in energy absorption / dissipation).

## **8. Dynamic Modeling – Runtime Reduction Testing**

The dynamic model for these runs is identical to that described in *Dynamic Model Overview – Boundary Conditions* with the exception of using the above methods to assess runtime reduction. As such it is important to understand the requirements for removing noise in a run's timestep.

Timestep of an explicit run is generally defined by the amount of time taken for a wave at the speed of sound to propagate through the defining length of an element. From this definition, the smallest element's size is the critical limitation to increasing the timestep

without artificial means. Therefore within these runtime reduction tests, the minimum element size was kept constant for each model.

For completeness it should be noted that in an explicit analysis the timestep may change during the run depending on contact or constraint interactions. Additionally, the timestep may be adjusted using mass-scaling or direct control (user-defined minimum). While these methods are applicable, these are considered outside the scope of this report because direct timestep adjustment will vary between load rate and boundary conditions even within a model. These methods can be used in tandem with the analyzed methods. Note that care must be taken in manually adjusting timestep; a large timestep will cause excessive error.

### 8.1. Symmetric Building Block Analysis

Testing between 3d symmetrical building block and non-symmetrical evaluates a model that is 'lightly cleaned up' by toggling lines that cause very small elements to be meshed against a model with reflected elements. Both models were evaluated as part of the convergence study (using the same parameters). Models are compared at a mesh size of 3mm due to the run time required for the non-symmetrical tank. The only difference between these models is the lack of ports on the symmetrical model and a decrease in element size in non-toggled geometry regions as shown in Figure 27. Convergence criteria comparisons are shown in Table 7.

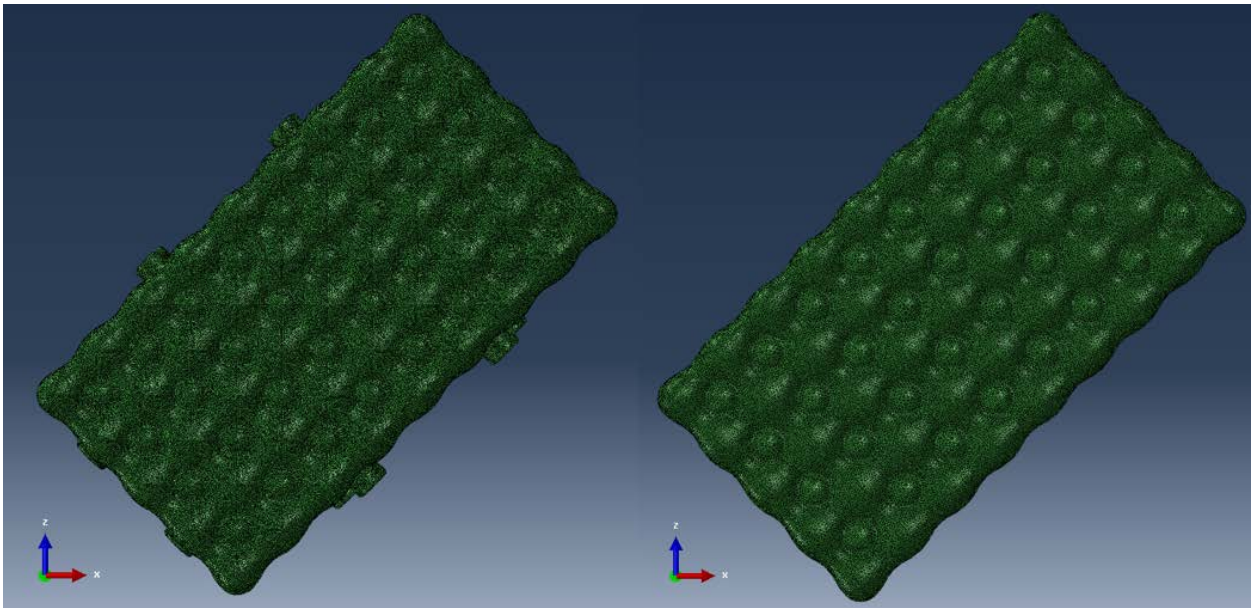


**Figure 27:** Non-Symmetric Model (left) and Symmetrically Built Model (right)

**Table 7:** Convergence Criteria and Run Time Comparing Non-Symmetric (with ports) and Symmetric Models

Model Style	Average Max Signed von Mises Stress, MPa	Recoverable Strain Energy, J	Internal Energy, J	CPU Run Time, hr:min
<b>Non-Symmetric Edge</b>	269.2	152.1	472.2	17:47:07
<b>Symmetric Edge</b>	259.9	152.5	467.5	3:03:24
<b>Error (%)</b>	3.4	0.31	0.98	82.8

In stress, there is a notable difference of 10 MPa between simulations. While this difference is within a 5% error, it is likely not solely due to numerical error. Instead, this increase in stress is likely due to the location of the ports. While the symmetric model has an equivalent kinetic energy this energy is spread equally across the tank. However, in the non-symmetric model this energy is applied at the ports which will slightly increase the bending moment applied to the impact edge. This bend is the cause of the maximum tensile stress in the model that increases the maximum tensile von Mises stress.

This conclusion is further supported by the maximum compressive stresses in the models which are 371.2 MPa and 370.9 MPa for the non-symmetric and symmetric edge runs respectively. Because the maximum compressive stress is a combination of bending and the impact itself, the compressive stresses are closer together than the tensile stresses. To fix this gap in maximum stress, it is recommended that the next set of building blocks include the ports. While this will take extra work, it will increase the accuracy of the results.

Looking at strain energy and internal energy, the values are within 1% and imply that the models are close enough to approximate each other. This gap with stress reemphasizes that stress should be tracked in convergence analyses.

As for run time, there is an 83% decrease in runtime by using the symmetric model. This decrease occurs due to the geometric fixes and mesh quality improvement prior to reflection. If the non-symmetric edge impact were to undergo the same improvements the run should take a similar amount of time. However, the time required to perform these fixes will increase as the tank size increases. In the building block method, only 1 piece needs to be fixed for each unique geometry while fixing the entire tank requires the same fixes to be applied to each piece.

This method is recommended for all CNG tank models, and any model with systematic fixes in geometry. The demonstrated runtime reduction for this model was roughly 83%. However, the primary gain from using this method is consistency in mesh quality and style.

## 8.2.Gradient Mesh Analysis

Gradient mesh analysis compares a '2.5 to X mm' gradient mesh to a baseline converged 2.5mm model where X is the defined final transition element size. The edge impact model is created by having a 2.5mm mesh along the edge as  $\frac{1}{4}$  of a core. The rest of the core is a 2.5mm to 'X' mm transition zone. Outside of this core, the model is meshed at 'X' mm. A figure demonstrating this mesh style is shown in Figure 28.

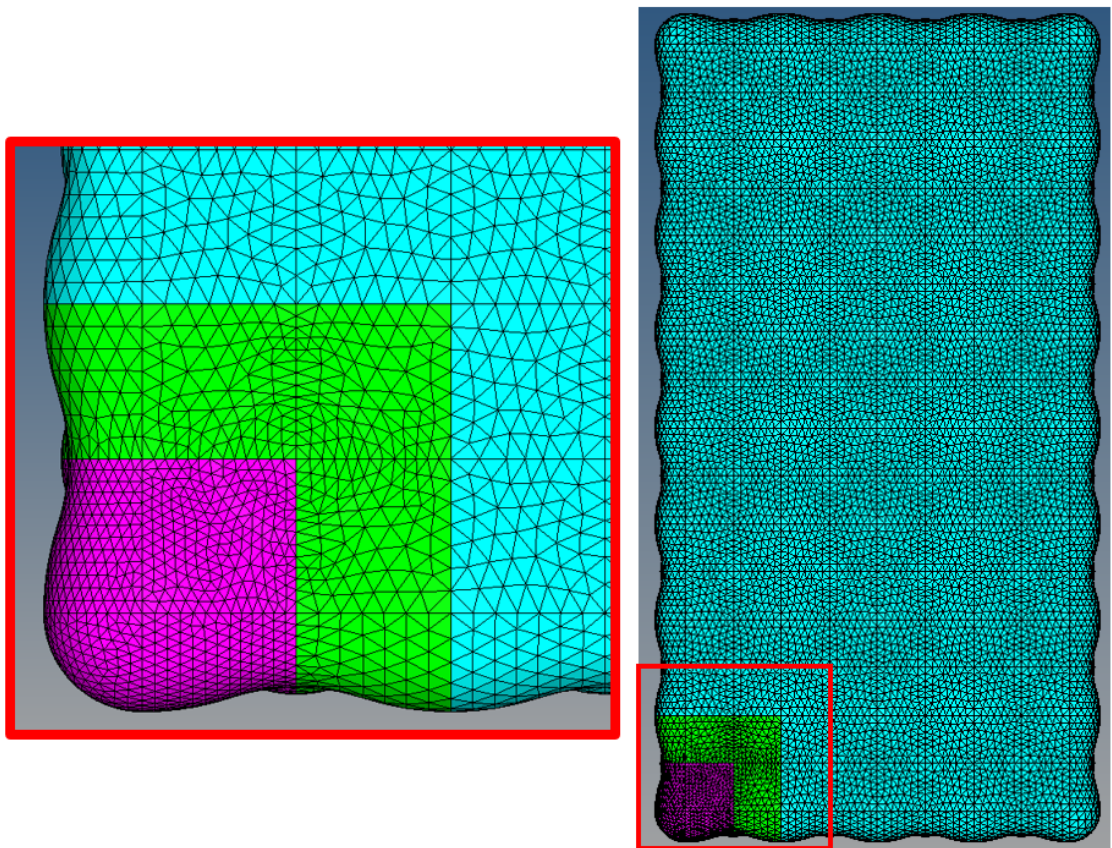


**Figure 28:** Gradient Mesh Transition; 2.5mm (Pink), 2.5 to 5mm (Green), and 5mm (Light Blue)

The rationale for where to begin the transition mesh is important. In this case the maximum stresses are all found within the first  $\frac{1}{4}$  core (pink). Therefore, the lower stresses outside of this region do not require a fine mesh. Using this information, the transition zone (green) was placed outside of this critical region. Without this distinction the method is not applicable.

Convergence results for the CNG tank edge impact are shown in Table 8 and Figure 29 respectively.

**Table 8:** Convergence Criteria and Run Time at Various Transition Element Sizes

Transition Element Size	Average Max Signed von Mises Stress (%Error), MPa	Recoverable Strain Energy (%Error), MPa	Internal Energy (%Error), MPa	CPU Run Time (%Change), hr:min
<b>2.5mm (Baseline)</b>	293.6 (0)	146.5 (0)	467.4 (0)	6:34 (0)
<b>3.5mm</b>	293.7 (0.03)	145.1 (0.9)	467.1 (0.05)	2:45 (58)
<b>4mm</b>	293.8 (0.07)	144.5 (1.3)	467.0 (0.08)	2:05 (68)
<b>4.5mm</b>	293.8 (0.07)	143.9 (1.7)	466.7 (0.15)	1:40 (74)
<b>5mm</b>	293.7 (0.03)	143.6 (2)	466.9 (0.1)	1:27 (78)

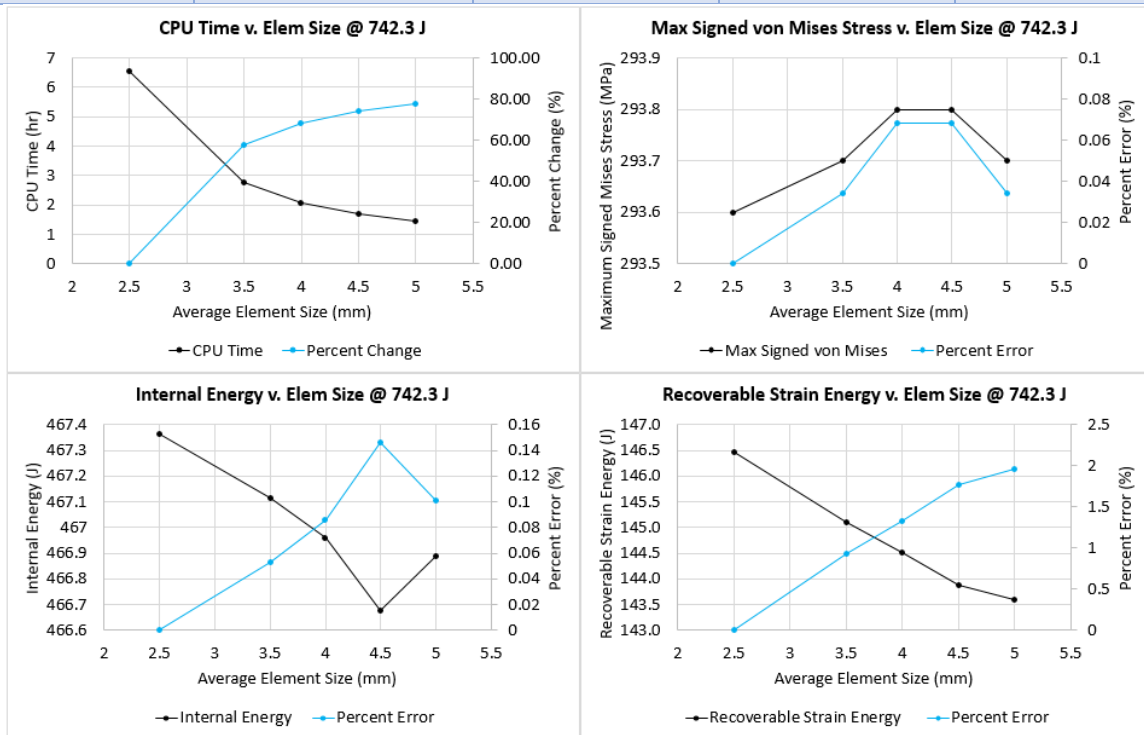


**Figure 29:** Graphed Convergence Criteria and Run Time v. Transition Element Size at Constant Initial Kinetic Energy (742.3 J)

While the graphs initially seem to indicate a large decrease in accuracy between runs it is important to note the scale of these points from Table 8. The stress results vary by less than 0.1% between tests. Similarly, all values of internal energy are within 0.15% of each other. The recoverable strain energy shows the largest difference between models which goes up to ~3 J difference between the baseline and final model and is an ~2% error. The closeness of these results implies that the gradient method is equivalent at all tested values of transition element size.

It is critical to note that this does not mean that any element size can be used as a transition size. The element sizes were limited to 5mm by measuring the aspect ratio of the transition elements. At 5.5mm element size, the transition elements exceeded an aspect ratio of 5. Therefore, the limitation on transition element size should be set by the user's quality criteria. However, this may allow for the user to continue the transition from 5mm to a larger element size assuming the mesh quality is still met.

Overall, the gradient mesh method is recommended for every model with non-critical stress locations. Using this method the runtime of edge impact models are shown to decrease by up to 78% on top of the gains displayed by the Symmetric Building Block method. This value should increase in corner impact tests because the entire edge does not need to be at the converged element size. Again, it must be noted that these tests are only considered valid after showing the gradient meshes do not deviate from the constant element size mesh. Therefore, this method is recommended for iterative runs where the runtime reduction can be utilized at least 1 subsequent model.

### **8.3.Hybrid Mesh Analysis**

Hybrid mesh analysis uses tetra elements for the external surface and 3-radius interface of the tank. For the internal surface there are multiple approaches; the entire internal geometry can be 2d, or a set number of cells can be 3d and the rest be 2d. Four different models are considered in this analysis: a model with 2d elements for the entire internal geometry (full 2d), a model with the impact cell meshed with 3d elements and the rest meshed with 2d elements (1 cell in), and a model with half the internal geometry meshed with 3d elements (half 2d). These 3 models are shown in Figures 30, 31, and 32 respectively.

An additional model was created using a combination of the gradient mesh and hybrid mesh styles. This model follows the '1 cell in' method but uses a gradient mesh from 2.5mm to 4mm to test the combined effect of the two methods. This '1 cell in gradient' model is shown in Figure 33.



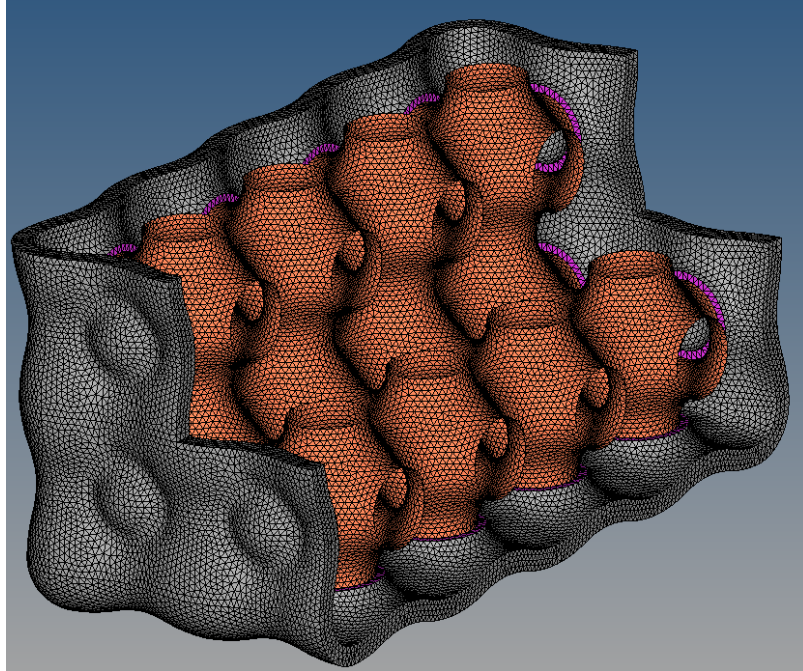


**Figure 30:** ‘Full 2d’ Hybrid Mesh Model – Impact Edge and Surrounding Cores

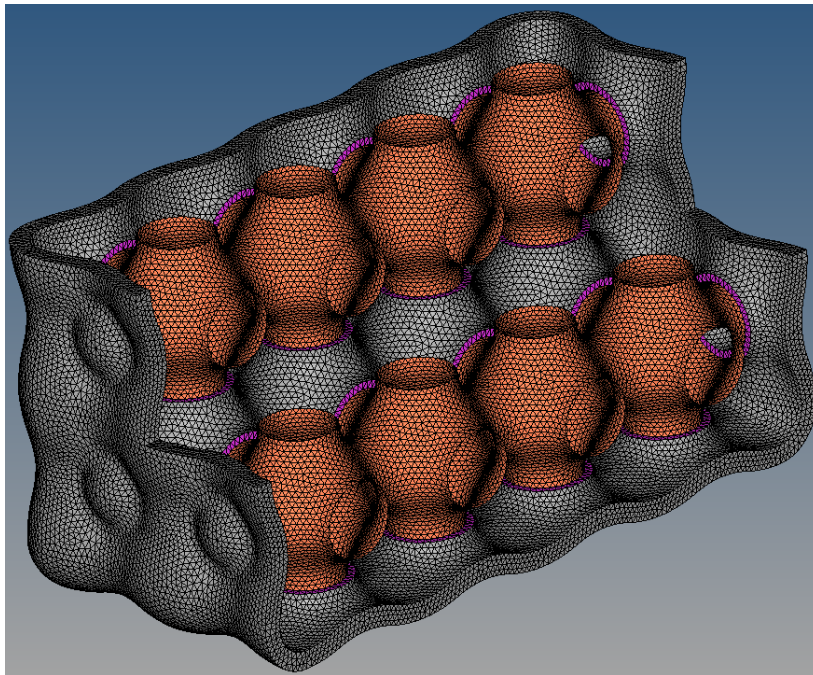


**Figure 31:** ‘1 Cell In’ Hybrid Mesh Model – Impact Edge and Surrounding Cores

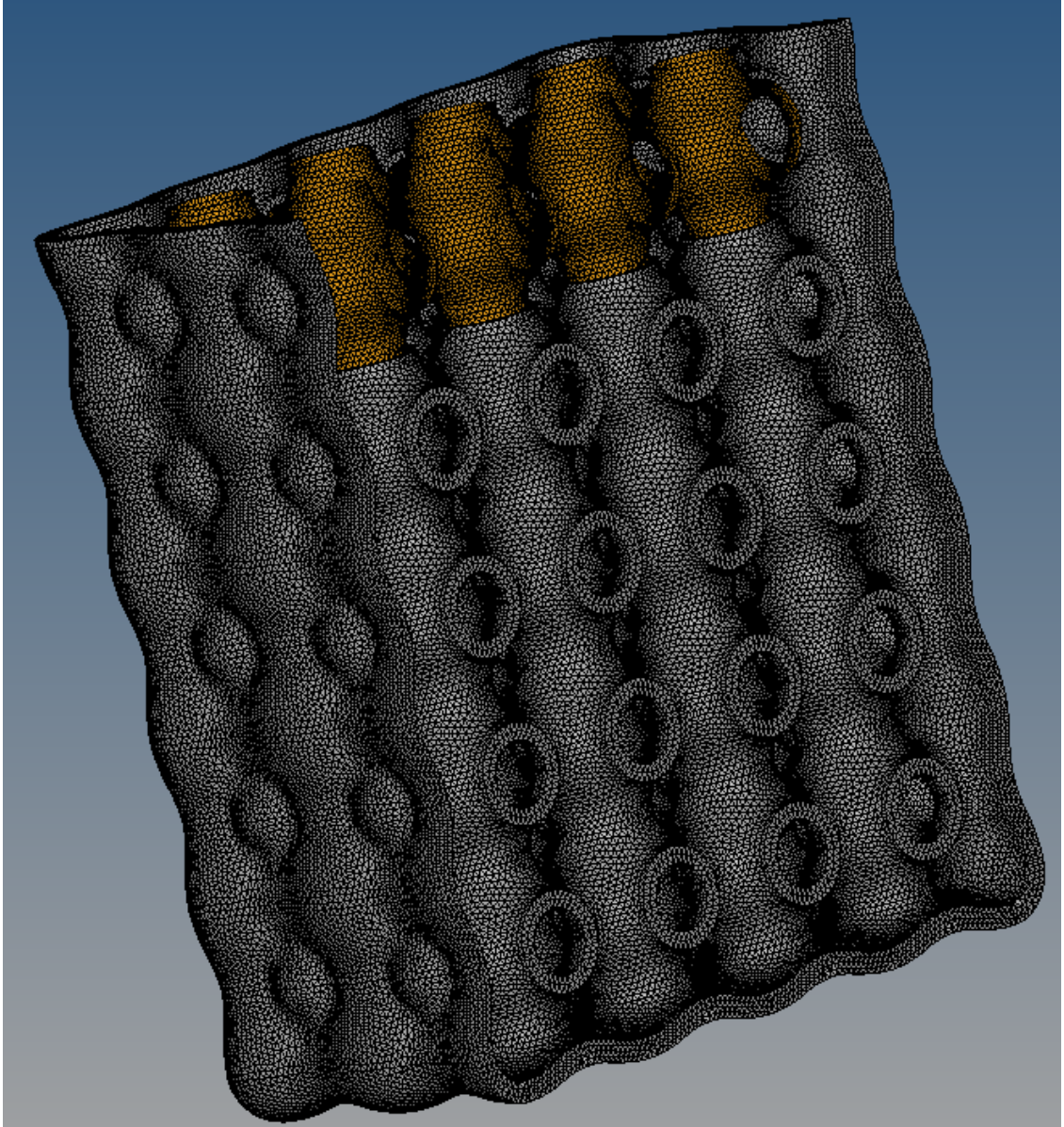


**Figure 32:** 'Half 2d' Hybrid Mesh Model – Impact Edge (lower left) and Mesh Transition



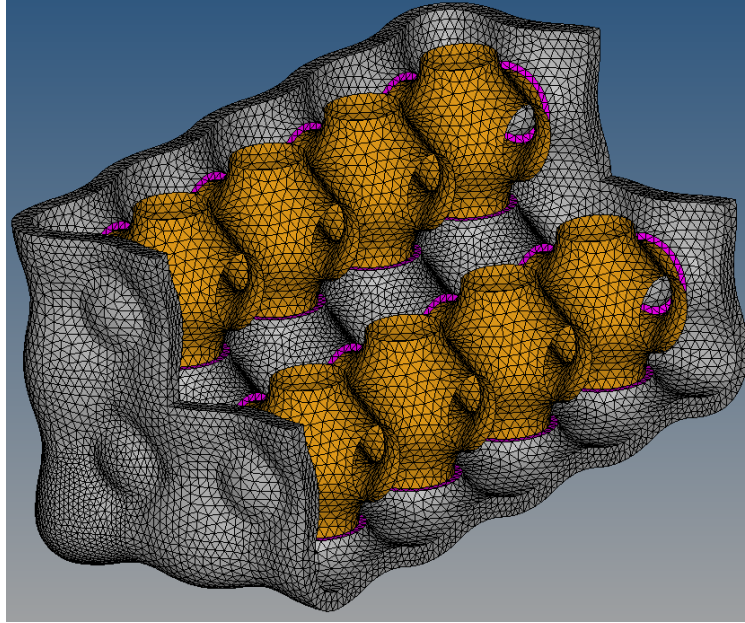


**Figure 33:** ‘1 Cell In Gradient’ Hybrid Mesh Model – Impact Edge and Surrounding Cores

The ‘full 2d’, ‘1 cell in’, and ‘half 2d’ models are designed to find where the transition region needs to be to create an accurate model. The ‘1 cell in gradient’ model is designed to understand the theoretical minimum time the model can run using the proposed methods. Convergence and runtime results for all 4 models and the baseline are given in Table 9.

**Table 9:** Convergence Criteria and Run Time for Hybrid Element Models

Model Name	Average Max Signed von Mises Stress (%Error), MPa	Recoverable Strain Energy (%Error), MPa	Internal Energy (%Error), MPa	CPU Run Time (%Change), hr:min
<b>Baseline (full 3d)</b>	293.6 (0)	146.5 (0)	467.4 (0)	6:34 (0)
<b>Half 2d</b>	330.3 (12.5)	150 (2.4)	453.7 (2.9)	7:56* (-32)
<b>1 Cell In</b>	346.2 (17.9)	150.1 (2.5)	461.8 (1.2)	5:25* (9.9)
<b>Full 2d</b>	346.6 (18)	150.85 (3.0)	462.1 (1.1)	5:45* (4.3)
<b>1 Cell In Gradient</b>	346.6 (18)	149.37 (2.0)	461.6 (1.2)	2:08* (65)

In these cases the max signed von Mises stress shows that the hybrid mesh method used is not applicable with the current connections between 2d and 3d elements. It should be noted that the unsigned von Mises stress does not vary from the max von Mises stress of the baseline model. This further proves that signed von Mises stress should be considered in the convergence criteria.

The reason for this discrepancy in maximum stress is attributed to the transition regions in the hybrid models. Because the connection elements cannot match the external geometry (via thickness property), the bending stiffness of these elements is lower than the actual bending stiffness in the tank.

The energy results all show below 3% difference in internal and recoverable strain energy. These results are both small compared to the typical 5% statistical standard for significant difference. In fact, these are large relative to the changes in energy seen in the gradient models and in convergence testing. This supports the conclusion that the current method of hybrid meshing does not properly replace the full 3d model. Additionally it supports the conclusion that energy measures should not be the only consideration for convergence of an FEA model.

The CPU time results show a minor decrease in run time when using a constant element size and a slight increase in run time as the number of tetra elements increases in the model. The reason for this is the timestep itself. In the hybrid models, Abaqus uses the minimum timestep from all elements (in this case  $9.54e-5$  ms). However, in the tetra models, the timestep is almost twice this value ( $1.78e-4$  ms). Because the tetra models can be run at a larger timestep it can be inferred that the hybrid mesh can also be run at this timestep, reducing the run time.

With a user-defined timestep equal to the tetra mesh timestep, the hybrid models would significantly reduce the run time of the model. This is especially true of the '1 cell in gradient' model which would reduce the run time to approximately 1 hour instead of 2.

The '1 cell in gradient' model shows minimal difference from the '1 cell in' model (less than 0.5 MPa and 0.5 J) and reduces the run time by more than a factor of 2 (50%). This is promising for combining the two methods if a valid hybrid mesh can be created.

Overall, the hybrid mesh must be fixed before further conclusions can be made on potential time reductions.

## **9. Conclusions and Recommendations**

Overall, convergence study results imply that, if a concrete slab is used, edge impact should be the driver for convergence. This report found that a mesh size of 2.5mm is an acceptable size to stay below 10 hour runs during optimization of the tank.

Additionally, it is recommended that convergence criteria includes signed or unsigned von Mises stress along with strain energy criteria. This allows the user to better understand the physical implications of the convergence results.

The recommended methods to use for reducing model run time is the Symmetric Building Block method and gradient meshing. These methods should be combined both to improve consistency in geometry fixes and ensure that a valid transition region is selected.

The Symmetric Building Block method should be performed by taking the primary parts required to build the CNG tank, fixing their geometry and combining them into the proper parts manually. This method is primarily based upon reflection and therefore does not require a large amount of time. Results from the *Symmetric Building Block Analysis* section indicate that, while ports were initially ignored, they should be included in the building blocks to avoid small errors in maximum signed von Mises stress. This meshing method reduced model runtime by 84% in the tested models. However, this reduction will fluctuate depending on the amount of time the user spends attempting to fix the entire tank if the method is not used.

The gradient mesh method should be performed after an initial (uniform element size) model of the tank has been run to determine a valid element transition starting point and baseline model. The mesh must maintain the user's minimum element quality at all times during the transition. For the edge impact condition, this transition was valid outside of the  $\frac{1}{4}$  core where maximum stresses occurred. It is recommended that the user measure convergence criteria for all gradient models to ensure the model does not vary much from the baseline model. Gradient meshing showed a runtime reduction of up to 78%. This gain should be larger for corner impact.

Hybrid meshing in the style used in this report shows promise for reducing runtime by an additional 50% on top of that indicated by gradient meshing with user-defined timestep control (though no reduction occurs if timestep is not set to the value in non-hybrid models). However, the meshing style used was not valid for maximum signed von Mises stress convergence criteria and must be fixed before usage in any optimization runs.

## **10.Potential Future Work**

Future work in time-reduction methods should focus on hybrid meshing and mass-scaling or user-defined timesteps.

Hybrid meshing work may require user-defined elements or some other element type that can fully transfer stresses from 3d to 2d elements. If a hybrid meshing method could be used, there is a high potential to further reduce runtime.

Mass-scaling or user-defined timesteps should be worked into impact analyses rather than studied directly. These methods typically are model and element dependent and will

likely shift between element sizes and geometries. This is especially true in the case of potential thickness optimizations.

If further work must be done in increasing accuracy for high deformation loading conditions, the material model in compression should be used to predict deformation. Methods such as adaptive remeshing may need to be included if elements deform out of acceptable tolerance.

## References

- [1] *More than 35% of U.S. Public Transit Buses Use Alternative Fuels or Hybrid Technology* [Online]. Available: [http://www.apta.com/mediacenter/pressreleases/2013/Pages/130422\\_Earth-Day.aspx](http://www.apta.com/mediacenter/pressreleases/2013/Pages/130422_Earth-Day.aspx)
- [2] *Congress Passes Continuing Resolution into New Administration* [Online]. Available: <http://www.apta.com/gap/legupdatealert/2016/Pages/Congress-Passes-Continuing-Resolution-into-New-Administration.aspx>
- [3] *Alternative Fuels Data Center: Maps and Data - Clean Cities Alternative Fuel and Advanced Vehicle Inventory* [Online]. Available: <http://www.afdc.energy.gov/data/10581>
- [4] *Alternative Fuels Data Center: Natural Gas* [Online]. Available: [http://www.afdc.energy.gov/fuels/natural\\_gas.html](http://www.afdc.energy.gov/fuels/natural_gas.html)
- [5] *Large Diameter CNG Cylinder* [Online]. Available: <http://www.government-fleet.com/channel/natural-gas/product/detail/2015/05/large-diameter-cng-cylinder.aspx>
- [6] *CNG United* [Online]. Available: <https://www.cngunited.com/cng-tanks-2/>
- [7] *CNG Tanks* [Online]. Available: <http://www.cngschool.com/cng-tanks>
- [8] *Conformable Compressed Natural Gas Tank* [Online]. Available: <http://www.relinc.net/advanced-materials/conformable-natural-gas-tank/>
- [9] L. Gambone, “Overview of NGV Fuel Tank Testing Requirements” CSA Group, Nov 18, 2013. [Online]. Available: [https://www.arpa-e.energy.gov/sites/default/files/documents/files/6\\_SessionA\\_Gambone\\_0.pdf](https://www.arpa-e.energy.gov/sites/default/files/documents/files/6_SessionA_Gambone_0.pdf)
- [10] *Concrete Slab Thickness* [Online]. Available: [http://www.engineeringtoolbox.com/thickness-concrete-slabs-d\\_1481.html](http://www.engineeringtoolbox.com/thickness-concrete-slabs-d_1481.html)
- [11] *Abaqus 6.14* [Online]. Available: <http://129.97.46.200:2080/v6.14/>
- [12] *Concrete – Properties* [Online]. Available: [http://www.engineeringtoolbox.com/concrete-properties-d\\_1223.html](http://www.engineeringtoolbox.com/concrete-properties-d_1223.html)
- [13] *Abaqus: Lecture 4 Contact Modeling* [Online]. Available: <http://imechanica.org/files/14-contact.pdf>